Sensitivity of the Paleocene-Eocene Thermal Maximum Climate to Cloud Properties

Journal:	*Philosophical Transactions A*
Manuscript ID:	RSTA-2013-0093
Article Type:	Research
Date Submitted by the Author:	24-Jan-2013
Complete List of Authors:	Kiehl, Jeffrey; National Center for Atmospheric Research, Shields, Christine; National Center for Atmospheric Research, Climate and Global Dynamics
Issue Code: Click here to find the code for your issue.:	DM1011
Subject:	Climatology < EARTH SCIENCES
Keywords:	climate change, equable climate, PETM, climate sensitivity

SCHOLARONE™
Manuscripts

Sensitivity of the Paleocene-Eocene Thermal Maximum Climate to Cloud Properties

By Jeffrey T. Kiehl*[1] and Christine A. Shields[1]

[1]*National Center for Atmospheric Research*
1850 Table Mesa Drive
Boulder, CO 80305

* Author for correspondence (jtkon@ucar.edu)

The Paleocene-Eocene Thermal Maximum (PETM) was a significant global warming event in Earth's history (~ 55 Ma). The cause for this warming event has been linked to increases in greenhouse gases, specifically carbon dioxide and methane. This rapid warming took place in the presence of the existing early Eocene warm climate. Given that projected business-as-usual levels of atmospheric carbon dioxide reach concentrations of 800 to 1100 ppmv by 2100, it is of interest to study past climates where atmospheric carbon dioxide was higher than present. This is especially the case given the difficulty of climate models in simulating past warm climates. This study explores the sensitivity of the simulated pre-PETM and PETM periods to change in cloud condensation nuclei (CCN) and microphysical properties of liquid water clouds. Assuming lower levels of CCN for both of these periods leads to significant warming, especially at high latitudes. The study indicates that past differences in cloud properties may be an important factor in accurately simulating past warm climates. Importantly, additional shortwave warming from such a mechanism would imply lower required atmospheric CO_2 concentrations for simulated surface temperatures to be in reasonable agreement with proxy data for the Eocene.

Keywords: climate change; equable climate, Paleocene Eocene Thermal Maximum; aerosol-cloud climate sensitivity

1. Introduction

Simulating warm climates of Earth's past has been a challenge for the climate modeling community for decades [1-2]. Using proxy estimates of atmospheric greenhouse gas concentrations in fully coupled climate models yields simulated polar temperatures that are often too cold, see e.g. [3] for a multi-model comparison with proxy data. An additional challenge is to warm the polar regions without excessively warming the equatorial region [2], a problem that exists in spite of polar feedback processes operating in the climate system. Simulating past warm climates with a fully coupled general circulation model is of great importance given the current and projected rise in atmospheric carbon dioxide, CO_2. Projections indicate that if humans continue to burn fossil fuels at the current rate, then atmospheric CO_2 levels will reach 800 to 1100 ppmv by the year 2100 [4-5]. It has been tens of millions of years since these concentrations of CO_2 have existed in Earth's atmosphere. There are certainly clear differences between the PETM climate state and the present and projected near future climate warming. Despite these significant differences, there is still a need to better understand how Earth's climate processes function in differing climate regimes. Thus, studying Earth's warm past climates such as the Paleocene Eocene Thermal Maximum (PETM) provide rich observational and modeling opportunities to better understand how Earth operates in an warm climate regime [6-7].

Over the years many physical mechanisms have been proposed to solve the low equator-to-pole thermal gradient problem in climate models. The basic challenge has been to find means of warming the polar regions more than warming the tropics under Eocene conditions (i.e. in the absence of strong snow and sea-ice and terrestrial ice feedbacks), since solely increasing greenhouse gases significantly warms both equatorial and the polar regions, e.g. [1]. Past

proposed climate mechanisms include: increased ocean heat transport [8], polar stratospheric

clouds related to enhanced atmospheric methane [9], increased deep cloud convection at high

latitudes with associated longwave cloud radiative forcing [10] and opening passage ways in the

Arctic [11], to name a few. It also has been argued that tropical temperatures may have been

higher than previously considered, which would allow for a purely enhanced greenhouse gas

explanation for warmer climates [2, 12-13].

The present study explores the role of another mechanism that may have operated in the

deep past. It has been pointed out that aerosol properties were no doubt significantly different in

deep time [14]. Specifically, Kump and Pollard [14] considered the role of reduced cloud

condensation nuclei (CCN) for the warm equable climate of the Cretaceous. They found that

lower levels of CCN led to a considerable warming of polar regions relative to warming in the

tropics due to associated changes in cloud properties. The present study presents results from a

coupled climate model that explores the possible roles of enhanced greenhouse gas

concentrations and sensitivity to reduced cloud condensation nuclei (CCN) for pre-PETM and

PETM climates. The exact properties of aerosols in the Eocene relative to the present are

unknown. However, given that the climate of the Eocene was very different than today, it likely

that aerosol properties were different, since aerosol properties are tied to phenomena such as:

vegetation type and distribution (organic aerosols, biomass burning), desert regions (dust

aerosols), surface wind patterns (sea-salt aerosols) and the ocean productivity (emissions of

DMS). Thus, the motivation here is to perform a sensitivity study to see if aerosol-cloud effects

could play an important role for the climate of the Eocene.

Here, present day observations from pristine regions (i.e. regions far from human

pollution, but still effected by natural sources) are used to constrain cloud properties, given that

currently there are no observations to accurately constrain Eocene aerosol properties. The study

also explores the sensitivity of the results to the assumed drop number concentration over

continents, since, even in present day conditions, there is an observed difference in natural

aerosols from marine to continental regions. Note that we are not suggesting that the Eocene had

aerosol properties identical to the modern pristine values. We are using the modern pristine

aerosol properties as a sensible starting point for this sensitivity study.

Additionally, reduction in low level cloud cover due to lower CCN leads to increased

shortwave heating of Earth's surface, which has important implications for estimates of global

carbon cycle budgets for past warm climates. Presently, models assume high CO_2 concentrations

that enhance Earth's greenhouse effect and warm the climate system. If aerosol-cloud effects

were significantly different in the past, then less carbon dioxide would be required to create a

similar warm climate state. This is significant, since assumed CO_2 levels for past warm climate

are often higher than those estimated by carbon cycle modeling [Pagani et al. 2006].

This study uses the fully coupled atmosphere-ocean-land-sea ice Community Climate

System Model (CCSM3) configured for the early Eocene paleoclimatic conditions. Simulations

are presented for climate conditions representative of both pre-PETM and PETM time periods.

The PETM simulation represents climatic conditions for the peak of the warming event, while

we use the term, PRE-PETM, for the simulation representing conditions prior to the warming

event. The present study does not attempt to simulate the temporal transition across the event due

to computational limitations in carrying out a simulation extending for tens to hundreds of

thousands of simulated years.

The benefit of considering the early Eocene compared to periods in the deeper past is

that paleoproxy data for temperatures for this time period cover a significant latitudinal range.

These data provide extensive evidence for extreme warmth at high latitudes [15], with a very active hydrologic cycle [16]. All of these reconstructions are signatures of a very warm climate regime due to elevated greenhouse gases. The data are also suggestive of mechanisms – positive feedbacks – that amplify the initial greenhouse radiative forcing [17-18].

The study is organized as follows: section 2 describes the model configuration and experimental design of the PETM and PRE-PETM simulations, section 3 presents the results from these simulations and compares simulated surface temperatures to various paleo proxy data, section 4 explores the implications of the present work for understanding Earth's sensitivity to increased levels of CO_2, section 5 summarizes the findings of the present study.

2. Model Configurations and Experimental Design

The present work employs the Community Climate System Model Version 3 (CCSM3) [19], a fully coupled climate model with active atmosphere, ocean, sea ice, and land components. Lengthy near steady state simulations require considerable computational resources so the low-resolution version of CCSM3 [20] is used for all simulations. The atmospheric and land components of the CCSM3 employ an Eularian spectral dynamical core of T31 (implying an equivalent horizontal resolution of 3.75^{o} x 3.75^{o}) with 26 vertical levels in the atmosphere. The ocean and ice components use a nominal 3° horizontal resolution with 25 oceanic depth levels. Further modifications include a marginal sea parameterization over the Arctic Ocean basin to ensure reasonable salinity values over long equilibrium runs (see [21] for further details). The equilibrium climate sensitivity of this version of the model is 2.5°C warming for a doubling of CO_2 from present day CO_2 concentrations. This sensitivity is on the lower end of the canonical

range of 2.1 to 4.5 °C [4] in climate sensitivity. Using a model with higher climate sensitivity

would require lower greenhouse concentrations to arrive at a similar climate simulation.

The model configuration employs recent reconstructions [21-22] of the middle Eocene

paleogeography, paleotopography and ocean bathymetry. Specification of the spatial distribution

of vegetation follows [22]. The vegetation specification is the same for both PRE-PETM and

PETM simulations, i.e. there is no vegetation feedback across the PETM event. Recent studies

suggest carbon dioxide levels for the PETM that may lie in a range from $\sim$ 1700 to 2250 ppmv

[23-24]. But it is fair to state that wide uncertainty exists in the actual CO_2 concentration during

both PRE-PETM and PETM climate states. Increases in atmospheric methane concentrations

have also been proposed for the PETM because of the observed negative carbon isotope

excursion in δC^{13} (see figure 3 in [25]). The assumed PETM atmospheric concentrations of CO_2,

CH_4 and N_2O are 2250 ppmv, 16 ppmv and 275 ppbv, respectively. The level of atmospheric

CO_2 is based on the work in [24] (L. Kump, personal communication), which used a

geochemical model of intermediate complexity to infer atmospheric CO_2 levels consistent with

geochemical markers. The level of CH_4 employed for the present work comes from a modeling

study on the effects of methane release during the PETM [26]. The PRE-PETM atmospheric

concentrations of CO_2, CH_4 and N_2O are 1375 ppmv, 760 ppbv and 275 ppbv, respectively. The

PRE-PETM level of CO_2 was obtained by taking the PETM simulation and reducing CO_2 levels

until the global annual mean temperature was reduced by $\sim$5 °C in order to agree with the global

estimate of observed temperature change. Here the use of a pre-industrial level of atmospheric

CH_4 is no doubt low for the warm early Eocene, given the moister environment that would have

allowed for more wetland regions. Given that there are no observational data to constrain

methane concentrations for this time period, a conservative assumption is made concerning the

PRE-PETM CH_4 levels. Note that sustained levels of methane require a continual release source of CH_4 into the atmosphere given the relatively short methane lifetime of ~12 years. This issue is addressed in section 4.

The change in cloud condensation nuclei was incorporated into the atmospheric model by altering both the liquid cloud drop number and effective cloud drop radii. As noted, there are no observations of cloud condensation nuclei or cloud microphysical properties for deep time periods. Thus, the present study should be viewed as a sensitivity study with regards to the effects of cloud microphysical properties on past climates. Framed as a sensitivity study, this work will make simple assumptions about aerosol and cloud properties for the Eocene. Given this assumption, an observational composite (see figure 5 in [27]) of cloud drop number for present day remote pristine regions is used to set the cloud drop number in the simulations. For present day pristine regions, the observed cloud drop number concentration is around 50 drops per cm^3 for liquid water clouds. Lower CCN leads to fewer cloud drops that grow to larger sizes. Observations indicate that effective cloud drop radii for pristine clouds are ~17 microns. For the sensitivity studies, the model configurations assume that all liquid clouds have present day pristine cloud drop properties. Once these properties are prescribed the cloud microphysical and radiative parameterizations in the atmospheric model respond to these cloud drop properties, i.e. cloud rainout processes and shortwave absorption change due to the change in cloud drop properties. Decreasing cloud drop number leads to increased precipitation rate and shorter cloud lifetime, which in the time mean implies a reduction in cloud cover. Increased cloud drop size leads to more shortwave absorption in clouds, which dissipates clouds. Fewer low level clouds results in more shortwave radiation reaching the surface. Since low level liquid water stratiform

7

clouds predominate at high latitudes, the reduction in these types of clouds leads to a preferential warming of polar regions.

To summarize, for PRE-PETM and PETM simulations, liquid water cloud properties are changed as follows: the cloud drop density is set to 50 cm^{-3} everywhere, as compared to the present day prescription of 400 cm^{-3} for continental regions, 150 cm^{-3} for ocean regions and 75 cm^{-3} over sea-ice and snow covered regions. The effective liquid cloud drop radius is set to 17 microns everywhere, as compared to the present day assumed values of 8 microns over land and 14 microns over ocean, sea-ice and snow covered regions. The role of continental versus marine cloud drop differences is explored in a companion PETM simulation in which the cloud drop density is set to 400 cm^{-3} and the cloud drop effective radius to 10 microns over continental regions.

All simulations employ a constant uniform pre-industrial aerosol optical depth representing a general background aerosol concentration. The simulations also assume a fixed geothermal heat flux into the oceans of 0.088 Wm^{-2}. All simulations assume a 0.487% reduction in solar luminosity for the early Eocene time period and the orbital parameters are those used in [21].

(a) Slab Ocean Model Sensitivities

Based on these modeling assumptions, four factors account for the warm simulated climate of the Paleocene Eocene Thermal Maximum (PETM): enhanced CO_2 concentrations, enhanced CH_4 concentrations, the absence of ice sheets and a reduction in cloud condensation nuclei (CCN), i.e. lower liquid cloud drop number and larger cloud drop effective radius. In order to assess the relative warming contribution from three of these factors – CO_2, CH_4 and CCN effects - sensitivity climate simulations were carried out with a version of the CCSM3 that

uses a slab mixed layer ocean component in place of the full dynamical ocean. Note that all of

these simulations assume the absence of terrestrial ice sheets and use the paleogeography of the

middle Eocene. In this version of the model the ocean heat transport for the mixed layer model is

based on the fully coupled PETM simulation. The advantage of the slab ocean model for

sensitivity studies is that it can be run to a steady state within only 40 simulated years. In the first

simulation, only CO_2 levels were decreased to a pre-industrial value of 280 ppmv. In the second

simulation, only CH_4 levels were decreased to a pre-industrial level of 760 ppbv. In the third

calculation, cloud drop number and effective drop radii were changed to present day (i.e.

polluted) values. The change in annual zonal mean surface air temperature from these three

simulations (figure 1a) indicates that the largest warming effect is due to CO_2 with polar

warming of 12 °C. The second largest warming is due to changes in CCN induced liquid water

cloud properties and yields a 7 to 9 °C warming at the poles, while the third largest contributor to

warming arises from increased CH_4 with a modest 4 °C warming at the poles. In order to

eliminate the effects of a different base state for these results, the normalized change in zonal

mean surface air temperature is shown (figure 1b), in which the zonal mean changes are

normalized by their respective global mean changes. If, similar amplification processes are

present in all three simulations, then the three curves should cluster together. However, in the

northern hemisphere polar regions, there are still significant differences between the CCN

simulation and CO_2 and CH_4 simulations. These differences are due to the inherent differences in

radiative forcing for the CCN simulation compared to the greenhouse gases simulations. The

radiative forcing from the CCN sensitivity simulation arises from two factors: 1) changing the

cloud drop number to 50 cm^{-3} lowers the liquid water path in the clouds and decreases cloud area

(this effect arises from an increase in precipitation efficiency and hence a decrease in cloud

lifetime), 2) increasing the cloud drop size to 17 microns decreases the single scattering albedo of the clouds, which leads to more shortwave absorption in the clouds. This, in turn, leads to a burn off of low cloud cover. Both of these effects result in more shortwave radiation reaching the surface. Additional simulations have been performed to isolate these two cloud effects to see which dominates high latitude warming. These simulations show that the change in cloud drop size – enhanced shortwave cloud absorption – dominates the CCN forcing simulations. At high latitudes, the CCN effect will play a major warming role during late spring though early fall, i.e. when shortwave radiative forcing is high. However, at high latitudes during local winter conditions, the shortwave CCN effect will not be active. Analysis of the simulations indicates that high latitude local winter warming is due to three factors: 1) an overall increase in tropospheric water vapor leading to an enhanced greenhouse warming, 2) an increase in upper tropospheric cloud cover leading to an increase in longwave cloud forcing, and 3) an open Arctic ocean basin that stores more energy through the winter as compared to an ice covered Arctic, which does not store energy through local winter. These results indicate that there are differences in response from the CCN effect compared to the standard greenhouse effect. This is essentially due to the fact that the CCN effect is affecting low level stratiform cloud cover, which predominate the high latitudes coupled with the seasonal asymmetry in solar radiation reaching high latitudes. These two factors lead to higher forcing at high latitudes compared to what is obtained from greenhouse forcing.

(b) Fully Coupled Simulations

The fully coupled PETM simulations involved a multi-stage spin up process. First, an initial PETM simulation was carried out by running the fully coupled CCSM3 for 600 years off of an ocean only simulation that had been run in an accelerated mode for 8300 years. This was

done in order to obtain a more representative deep ocean state. The PRE-PETM fully coupled

model was run from this simulation with the PRE-PETM CO_2 and CH_4 concentrations and

pristine CCN conditions. The PRE-PETM state was run for another 1400 years. The ocean state

for this simulation has vigorous ventilation which means the deep ocean comes into an

approximate steady state. CO_2 and CH_4 concentrations were then set to their PETM levels and

the PETM simulation was initialized from the end of PRE-PETM simulation and run for another

1660 years, after which the net energy imbalance of the coupled PETM climate system was less

than 0.4 Wm^{-2}. Thus, the deepest layers of the ocean in this simulation are still not in a steady

state. However, the surface temperatures at the end of this simulation have reached near steady

state conditions with trends in zonal mean surface temperature less than 10^{-4} °C per year. All

results are based on 50 year averages from the end of the PRE-PETM and PETM CCSM3

simulations.

3. Model Results

(a) Simulated global mean state

The global annual mean sea surface temperature (SST) for the fully coupled PETM

simulation is 32.3 °C. To obtain an estimate of the observed PETM global mean SST, it is

assumed that the zonal surface temperature can be represented by the function $A + B \cos(\varphi_{lat})$,

where φ_{lat} is paleolatitude [5]. Two observational points [28, 29] at 36°N and 75°N paleolatitude

with SSTs of 33 °C and 25 °C, respectively, determine the coefficients A and B. Analytically

integrating the expression yields an observed estimated global annual mean SST of 33 °C for the

PETM. Thus, the simulated global annual mean SST is in good agreement with the first order

observational estimate. Note that the simulated global mean surface temperature (land plus

ocean) is 31.9 °C, so the SST value provides a very good estimate for the global mean. This

agreement between ocean only and global mean values is applicable in a warm world with little

snow or ice cover.

(b) Simulated ocean state

Zonal annual mean sea surface temperatures from the PETM and PRE-PETM model

simulations exhibit a reduced equator to pole temperature gradient compared to the present day

simulation (figure 2). Note that the present day CCSM3 simulation is in good agreement with

observed sea surface temperatures with a slight cold bias in the polar regions. As noted from the

slab ocean sensitivity simulations, the dominant factors contributing to the amplified polar

warmth are increased atmospheric CO_2 concentration and the change in cloud properties

associated with reduced cloud condensation nuclei (see figure 1). Increased levels of atmospheric

methane contribute one-third of the warming relative to warming from increased CO_2. Zonal

mean PETM sea surface temperatures at ~70 degrees north and south are ~ 20°C in good

agreement with the proxy estimates at these latitudes (see Table 1 for point wise comparisons

with proxy data). Tropical temperatures for the PETM are ~40 °C. Currently, there are no proxy

estimates of sea surface temperatures for the deep equatorial marine environment, but tropical

and subtropical temperatures approaching the PETM indicate a warm climate with surface

temperatures of in the range of 35 to 41 °C (see figure S1 in [2]).

The simulated spatial distribution of PETM tropical and sub-tropical sea surface

temperatures (figure 3a) is similar to the modern day pattern with a warm pool of water in the

Indian western Pacific Oceans and a cold tongue of water in the eastern Pacific. Warm pool

temperatures in excess of 40 °C exist in the paleo Tethys region on either side of India indicating

the lack of an ocean thermostat to keep these waters close to present day values. Warm waters

extend far into the extra-tropics with 32 °C water off the coast of present day New Jersey in good

agreement with the proxy data for this region [28] (Table 1). At higher latitudes, the PETM

Arctic is slightly cold by ~8 °C compared to the observational value for this region [29]. Note

that simulated PETM summer temperatures are in better agreement with the observational

estimate (Table 1). The largest discrepancy between simulated sea surface temperatures and

reconstructions occurs at 55 ° South latitude [30]. Here the model is colder than the proxy data,

but again the simulated summer temperature is closer to the observations. Further south at 65°

latitude the model agrees with the proxies to within 2 °C [31].

The change in sea surface temperature (figure 3b) (PETM minus PRE-PETM) is in good

agreement with observed changes at all latitudes (see Table 1 in [32] for a compilation of proxy

changes in SSTs). Given that the PRE-PETM model atmospheric CO_2 level of 1375 ppmv was

chosen to ensure a ~5 °C global annual mean change in surface temperature (see section 2), this

agreement may seem unsurprising. However, the choice of this CO_2 level does not guarantee that

the spatial distribution of change in temperature will agree with reconstructions at specific

geographic locations.

The sea surface salinity distribution for the PETM simulation (figure 4a) shows

extremely fresh waters in the Arctic basin, which is in agreement with recent published proxies

[16]. One important regional feature of the PETM simulation is high salinity located in the

Turgay strait between present day Europe and Asia. As will be shown below, this feature

increases surface water density relative to the PRE-PETM simulation causing sinking in this

region. The overall salinity distribution - determined by local water balance between evaporation

minus precipitation and runoff (figures 4b – 4c) - exhibits enhanced net fresh water input at high

latitudes compared to the present day climate and enhanced tropical precipitation. Continental

runoff plays an important role in determining salinity levels in coastal regions (compare figures

4a and 4c), where the largest runoff occurs into the Arctic basin and in the tropical regions.

The location and strength of deep water formation is important for understanding the

deep ocean circulation. In particular, changes in deep water formation due to increasing levels of

greenhouse gases may have important implications for carbon cycle processes [33-34]. The

seasonal cycle of maximum mixed layer depth (figure 5) is an informative measure of the

location of deep water formation. Other measures were also used to identify regions of deep

water formation occurring in the PRE-PETM and PETM simulations including the seasonal

cycle of surface potential density and isopleths of zonal potential temperature and salinity. The

conclusions concerning deep water formation using maximum mixed layer depth are supported

by all of the above metrics. Two winter months of maximum mixed layer depth for each

hemisphere are shown (figure 5), since these seasons are when the densest waters sink to

maximum depth. Northern hemisphere winter PRE-PETM maximum mixing (figure 5a-b) occurs

in the north Pacific, where water formed in this region penetrates to 4000 meter depth. Mixing is

very vigorous indicated by ideal water ages of < 50 years at these depths, where ideal age

measures the time in years that water at a specific depth was last exposed to the ocean surface. In

the southern hemisphere winter PRE-PETM (figures 5c – 5d), maximum mixing occurs off the

coasts of Australia and Antarctica. Again, ocean ventilation is very efficient for this region. This

efficient ventilation for the PRE-PETM climate means that the deep ocean is strongly coupled to

the ocean surface in high latitude regions. It also means that the equilibrium time scale of ocean

circulation for the PRE-PETM ocean state is much shorter than that of the PETM world. The

maximum mixed layer depths for the PETM simulation (figure 5e – 5h) exhibit a very different

configuration for deep water formation. The high latitude Pacific formation sites for both

hemispheres no longer exist. Surface warming and fresh water input at high latitudes have significantly reduced the specific density gradients and stratification has essentially shut off high latitude deep water pathways. However, one region of maximum mixed layer depth remains in the Turgay straight. Here high surface salinities (figure 4a) cause surface waters to sink to ~1000 meters depth. This water then spreads out from the Tethys region forming intermediate waters into the wider Pacific region. Thus, the source location of deep water formation switches in going from the PRE-PETM into the PETM climate state as first suggested by the modeling results of Bice and Marotzke (2001) [35] and proxy studies [36-38].

The effects of this shift in water mass formation is reflected in the ocean circulation at 1000 meters depth between the PETM state (figure 6a) and the PRE-PETM (figure 6b). These figures show a shift from a circulation with stronger and larger gyres to a weaker circulation for the warmer climate. Note that the gyre circulation is also due to a shift in the atmospheric circulation in moving into a warmer climatic state. Figure 6a also exhibits evidence for the flow of warmer water from the Turgay straight out to the Pacific in the PETM state as compared to PRE-PETM. The near surface PETM circulation (figure 7) exhibits surface flow from the Atlantic into the Pacific through the open Panama straight. The simulation also shows signatures of both Kurishio and Gulf – like currents along the eastern boundaries of present day Asian and North American continents, respectively. Coastal upwelling driven by along-shore atmospheric circulations is also apparent.

One proposed mechanism for maintaining a low equator to pole thermal gradient was related to an increase in ocean heat transport [8]. The present simulations find no evidence for this hypothesis (figure 8) in agreement with other modeling studies that have used fully coupled GCMs to study the warm Eocene [39]. Indeed, the warmer climate state of the PETM exhibits

less northern hemisphere ocean heat transport compared to either the PRE-PETM climate or the

present day simulated climate. Peak PETM ocean heat transport at 20 to 30° North is ~30% less

than PRE-PETM transport and ~45% less than present day peak transport. Note, however, that

ocean heat transport in the southern hemisphere is greater than the present day simulated

transport and may contribute to warmer high latitude temperatures in this region.

Finally, the zonal annual mean vertical thermal structure of oceans for both PETM and

PRE-PETM simulations (figure 9a and figure 9b) is significantly different than the present day

thermal structure (figure 9c). In general, the warm Eocene simulations are more stratified than

the present day ocean structure, in agreement with previous studies, e.g. [33, 39]. This

stratification is more evident when considering vertical profiles of potential temperature (figure

10 a-d) for tropical and northern and southern high latitude regions. For northern hemisphere

winter conditions (figures 10a-b), the PRE-PETM simulation shows a region in the north Pacific

of near constant temperatures through the depth of the ocean column, indicative of vigorous

mixing in this region. In the PETM state, this region of mixing is suppressed. Similarly, for the

southern hemisphere winter (figures 10c-d), a region of well-mixed water exists in the southern

Pacific, which has been suppressed in the PETM climate state.   The PETM ocean temperatures

at depths ranging from ~1300 to 3400 meters for specific locations are generally in good

agreement with proxy data (Table 2). However, it must be remembered that at these depths the

ocean state is still warming in the PETM simulation.

(c) Simulated terrestrial state

The simulated high latitude terrestrial annual mean surface air temperatures for the

PETM (figure 11a) are 15 to 20 °C, in reasonable agreement with the limited proxy data. For

example, temperatures for the Wyoming Bighorn Basin are in excellent agreement with

reconstructions (Table 1) [40]. Simulated surface temperatures in the tropical regions of South

America and Africa are excessively high, in excess of 48 °C at some points. Such high

temperatures would imply severe conditions for the existence of life in these regions. The change

in surface air temperature from PRE-PETM to PETM conditions (figure 11b) shows warming of

5 to 10°C for most regions. This 5-10°C warming in middle North America is very good

agreement with data [6]. For the northern most region of North America, minimum January

temperatures are 8°C, which is supported by the limited paleobotanical evidence of palm trees at

these high latitudes. In general, for the PETM simulation cold month mean surface air

temperatures are above freezing at all locations (figure 12a), while for the pre-PETM

intercontinental region cold month mean temperatures are below freezing (figure 12b). A

comparison of simulated terrestrial surface temperatures with the proxy compilation of Huber

and Caballero [12] (figure 13) indicates general agreement across a range of locations. Given

that the reconstructions span a wide range of early Eocene time periods, with few data

representative of the PETM event, agreement is expected to be better for the PRE-PETM

simulation compared to the PETM and indeed this is the case (compare figures 13 a and b,

respectively).

        As noted in the introduction, specification of a continental cloud drop size density of 50

cm^{-3} may be too low, given the diversity of aerosol sources from vegetation (secondary organics,

biomass burning) and changes in surface conditions, e.g. dust loading. An additional sensitivity

study was carried out to test how the PETM results depend on this assumption. Using a cloud

drop size of 400 cm^{-3} and drop effective radius of 10 microns over continental regions (figure 14)

leads to a 2 to 3 °C reduction in continental surface temperature. Thus, inclusion of a difference

between continental and marine CCN conditions slightly cools the continents relative to the

simpler approach of uniform CCN or cloud drop properties.

In general, the hydrologic cycle over land is enhanced in the PRE-PETM and PETM

simulations compared to the present day simulation as reconstructions suggest [41]. Runoff in

the Arctic also increases from the PRE-PETM to the PETM resulting in very fresh water for the

entire basin a feature of the Arctic supported by proxy data [16]. Overall the hydrologic cycle is

more vigorous for the warm Eocene simulations compared to the present day simulation. The

change in precipitation over land (figure 15) from the PRE-PETM to the PETM climate state

indicates that most regions experience an increase in rainfall. In the northern part of North

America, precipitation increases by 20 to 50%. However there are locations that experience a

slight reduction in precipitation, e.g. the North American southwest. Reconstructions of changes

in precipitation [40] in North America offer a complex picture of regions of decreased

precipitation early after the event, but general increase in precipitation at the peak of the warm

PETM. The seemingly large percentage change in precipitation in the central African region is

somewhat misleading given that both the PRE-PETM and PETM simulated precipitation in this

region is very low (< 1 mm d^{-1}). The percentage change in this general region of low

precipitation appears to be related to the poleward shift in the zonal mean circulation, which

affects moisture transport into this region.

4. Implications for Climate Sensitivity

Considerable attention has recently been given to what deep time climates tell us about

Earth's climate sensitivity [5, 42-44]. The traditional or Charney climate sensitivity is defined as

the equilibrium warming due to a doubling of carbon dioxide about the modern climate state and

assumes that the factors amplifying the initial greenhouse radiative forcing take place on time

scales of days to decades. Thus, this sensitivity includes feedback mechanisms involving changes

in processes such as water vapor, lapse rate, clouds, and sea-ice. One measure of the strength of

these feedback processes is the so-called climate feedback factor defined as the ratio of the

doubled CO_2 equilibrium warming (~2.5 °C) to the radiative forcing due to a doubling of CO_2 (~

3.7 Wm^{-2}), i.e. ~ 0.68 °C $(Wm^{-2})^{-1}$.

As discussed in section 3a, the present study arrives at a proxy estimate for the global

mean PETM surface temperature of ~33 °C. Given that Earth's pre-industrial temperature was ~

15°C, the PETM was warmer by 18 °C compared to the pre-industrial time period. Assuming

that the PETM CO_2 concentration (2250 ppmv) was eight times larger than pre-industrial levels

implies a CO_2 radiative forcing of 14.5 Wm^{-2}, where the CO_2 forcing is obtained by the method

described in [45] employing the atmospheric version of CCSM3 in a fixed SST configuration.

The shortwave forcing from pre-industrial to the PETM time period (55 Ma), due to the change

in solar luminosity, is a forcing of -1.2 Wm^{-2}, assuming a planetary albedo of 0.27 derived from

the PETM simulation. Thus, the net forcing (CO_2 greenhouse + solar luminosity) from pre-

industrial to the PETM is ~13 Wm^{-2}. Using these estimates for the PETM implies a feedback

factor of ~ 18 °C/(13 Wm^{-2}), or ~ 1.4 °C $(Wm^{-2})^{-1}$. Thus, the climate sensitivity considering a

change in state from the modern to the PETM is two times larger than the modern Charney

sensitivity. This larger climate sensitivity has been called the Earth System Sensitivity (ESS)

[41] and includes feedback processes operating on time scales of decades to many millennia,

e.g.: ice sheet destabilization, possible methane hydrate release, changes to vegetation and

alterations to the global carbon cycle. Note that if a lower PETM CO_2 concentration were

assumed, then the deduced ESS would be even higher.

Submitted to Phil. Trans. R. Soc. A - Issue

Page 20 of 47

What do the paleoclimate simulations of the PRE-PETM and PETM in this study have to say concerning the issue of an enhanced ESS over the Charney sensitivity? In addition to CO_2 forcing, the absence of ice sheets and paleogeography, this study considers two other factors to explain the warm simulated climates of the PRE-PETM and the PETM relative to the modern climate state: 1) increased methane concentrations, and 2) lower cloud condensation nuclei. This sensitivity study suggests that these two additional processes may have played a critical role in enhancing climate sensitivity on long time scales relative to the present day climate. Note that this argument assumes that methane release and changes in aerosol-cloud interactions operate as feedback mechanisms and not forcing factors on these long time scales.

With regards to methane, Dickens [18] has argued that release of large reserves of methane is quite feasible for the warm Eocene. Continued release of methane from expanded wetland regions containing bacteria would also have led to sustained levels of atmospheric methane [46]. Sustained emissions of methane would be required to maintain elevated CH_4 levels in the presence of an otherwise short lifetime.

With regards to changes in CCN, this study uses present day observations for very pristine regions to constrain the model cloud microphysical properties. This assumption is clearly simplistic given the temporal, spatial and chemical variability that exists in real aerosols. Thus, what is presented here is a sensitivity study, which uses present day knowledge to link CCN and cloud drop number density. Kump and Pollard [14] provided arguments for why CCN would have been lower during the warm Cretaceous. There may be other reasons for lower CCN during past warm climate states, some of which may be linked to atmospheric chemistry. A recent study [47] found that the production of aerosols actually decreases in the presence of certain types of vegetation. This effect is actually opposite to what occurs where the production of secondary

organic aerosols increases due to the emission of certain biogenic precursors from vegetation. The explanation of these new findings involves the effects of isoprene emissions from vegetation on the concentration of the atmospheric hydroxyl radical, which plays an important role in aerosol formation. In this case, increased warming initiated by increased greenhouse gases would lead to the migration of forests to higher latitudes [48] accompanied by a reduction in CCN with additional warming. This proposal is hypothetical, as such it would be of value to look for particular proxies that could either validate or invalidate this hypothetical biophysical feedback. Note that the conclusions presented here do not depend on this particular proposed mechanism, since this study considers the general sensitivity of the warm climate state to changes in cloud microphysical properties derived from present day pristine conditions.

To date, modeling past warm climates, such as the Eocene, has focused mainly on two climate factors: greenhouse forcing and enhanced climate sensitivity. For sufficiently high CO_2 concentrations, enhanced greenhouse forcing yields a warm climate approximating reconstructions. However, the assumed level of CO_2 may be too high compared to paleo pCO_2 proxies. Another solution to this dilemma is to use a model with a higher climate sensitivity, which means that a lower CO_2 concentration yields similar agreement with the reconstructions. The present work explores a third factor that is important to the climate system, i.e. shortwave forcing. This sensitivity study shows that including changes in shortwave forcing – via CCN-cloud interactions – results in additional heating of the climate system, which, in turn, implies that less CO_2 is required to produce a similar warm climate state. In light of these results, a CCN-cloud mechanism could help alleviate current disparities between assumed CO_2 levels in climate models and those estimated from carbon cycle budget models for past warm climates.

5. Conclusions

The present study finds that CCSM3 simulations of the PETM climate that includes enhanced levels of CO_2, CH_4 and lower cloud drop numbers are in good agreement with a wide range of paleo temperature records. Along with the studies in [12] and [13], this is one of the few coupled climate model simulations that agrees with much of the proxy data, including polar regions. The simulations show that the climate system is sensitive to the specification of reduced levels of CCN and associated changes in cloud properties. Hence, this may be an important climate factor that needs to be accounted for in simulating past climates. Given these findings, it would be of great value to find means to quantify the aerosol properties that may have existed in past climate states.

In support of previous studies and reconstructions, the study finds that the ocean general circulation shifted between the PRE-PETM climate to that of the PETM state. In particular, the sites of deep water formation shifted from the high polar regions in both hemispheres to the mid latitudes upon entering the warmer PETM climate. Simulated deep ocean temperatures agree well with the limited available data for the PETM. In terms of the terrestrial sites, the PETM simulation is in good agreement with much of the proxy data. Surface temperatures are not excessively cold, with cold month mean temperatures staying above freezing. The simulations also indicate that the hydrological cycles of the PETM and PRE-PETM were far more active then present day. In addition, the more active high latitude hydrological cycle led to an increase in fresh water input into the Arctic basin. Remaining questions are related to the magnitude of surface warming for marine and terrestrial regions in the tropics between 30 °S to 30 °N. Little data exists to constrain surface temperatures in this region. The model simulations suggest

surface temperatures in excess of 45 °C for certain regions. It is important to find stricter proxy constraints for these tropical regions.

Finally, this study supports the finding of others that Earth's climate system is more sensitive to greenhouse forcing on longer time scales, e.g. [42-44]. In particular, this work finds that the Earth System Sensitivity for the PETM or PRE-PETM relative to the modern climate is twice as large as the traditional Charney climate sensitivity.

23

References

1 Barron, E. J. 1987 Eocene equator-to-pole surface ocean temperatures: a significant climate

problem? *Paleoceanog* **2**, 729-739.

2 Huber, M. 2008 A hotter greenhouse? *Science* **321**, 353-354.

3 Lunt, D.J., Dunkley Jones, T., Heinemann, M., Huber, M., LeGrande, A., Winguth, A.,

Loptson, C., Marotzke, J., Tindall, J., Valdes, P. & Winguth, C. 2012 A model-data

comparison for a multi-model ensemble of early Eocene atmosphere-ocean simulations

EoMIP. Discussions in *Climate of the Past*, **8**, 1229-1273, (doi:10.5194/cpd-8-1229-2012)

4 Solomon, S., Qin, D., Manning, M., Chen, Z., Marquis, M., Averyt, K.M., Tignor, M. &

Millier, H.L. (eds) 2007 *Contributions of working group 1 to the fourth assessment report of*

the Intergovernmental Panel on Climate Change. Cambridge, UK; New York, NY:

Cambridge University Press.

5 Kiehl, J. T. 2011 Lesson's from Earth's past. *Science* **331**, 158-159.

6 McInerney, F.A. & Wing, S.L. 2011 The Paleocene-Eocene Thermal Maximum: A

perturbation of carbon cycle, climate, and the biosphere with implication for the future.

Annu. Rev. Earth Planet. Sci. **39**, 489-516.

7 NRC 2011 *Understanding Earth's Deep Past.* National Research Council, National Academies

Press, Washingon D.C.

8 Lyle, M. 1997 Could early Cenozoic thermohaline circulation have warmed the poles?

Paleocean. **12**, 161-167.

9 Sloan, L. C. & Pollard, D. 1998 Polar stratospheric clouds: a high latitude warming mechanism

in an ancient greenhouse world. *Geophys. Res. Lett*. **25**, 3517-3520.

10 Abbot, D. S., Huber, M. Bousquet, G., & Walker, C. C. 2009 High-CO_2 cloud radiative

forcing feedback over both land and ocean in a global climate model. *Geophys. Res. Lett.,* **36**,

L05702. (doi:10.1029/2008GL036703)

11 Shellito, C. J., Lamarque, J.-F. & Sloan, L. C. 2009 Early Eocene Arctic climate sensitivity

to pCO_2 and basin geography. *Geophys. Res. Lett*. **36** (doi:10.1029/2009GL037248)

12 Huber, M. & Caballero, R. 2011 The early Eocene equable climate problem revisited. *Clim.

Past* **7**, 603-633 (doi:10.5194/cp-7-603-2011).

13 Heinemann, M., Jungclaus, J.H. & Marotzke, J. 2009 Warm Paleocene/Eocene climate as

simulated in ECHAM5/MPI-OM. *Clim. Past*, **5**, 785-802.

14 Kump, L. R. & Pollard, D. 2008 Amplification of Cretaceous warmth by biological cloud

feedbacks. *Science* **320**, 195.

15 Sluijs, A., Shouten, S., Pagani, M., Woltering, M., Brinkhuis, H., Damste, J.S.S., Dickens,

G.R., Huber, M., Reichart, G-J., Stein, R., Matthiessen, J., Lourens, L.J., Pendentchouk, N.,

Backman, J., Moran, K. & the Expedition 302 scientists 2006 Subtropical Arctic Ocean

temperatures during the Paleocene/Eocene Thermal Maximum. *Nature* **441**, 610-613.

16 Pagani, M., Pedentchouk, N., Huber, M., Sluijs, A., Schouten, S., Brinkuis, H., Damste,

J.S.S., Dickens, G.R. & the Expedition 302 Scientists 2006 Arctic hydrology during global

warming at the Palaeocene/Eocene thermal maximum. *Nature* **442**, 671-675.

17 Pagani, M., Caldeira, K., Archer, D. & Zachos, J.C. 2006 An ancient carbon mystery. *Science*

314, 1556.

18 Dickens, G.R. 2011 Down the rabbit hole: toward appropriate discussion of methane release

from gas hydrate systems during the Paleocene-Eocene thermal maximum and other past

hyperthermal events. *Clim. Past* **7**, 831-846 (doi:10.5194/cp-7-831-2011).

19 Collins, W. D., Bitz, C.M., Blackmon, M.L., Bonan, G.B., Bretherton, C.S., Carton, J.A.,

   Chan, P., Doney, S.C., Hack, J.J., Henderson, T.B., Kiehl, J.T., Large, W.G., McKenna, D.S.,

   Santer, B.D. & Smith, R.D. 2006 The Community Climate System Model Version 3

   (CCSM3). *J. Clim.* **19**, 2122-2161.

20 Yeager, S.G., Shileds, C.A., Large, W.G. & Hack, J.J. 2006 The low resolution CCSM3. *J.

   Climate* **19**, 2545-2566.

21 Winguth, A., Shellito, C., Shields, C. & Winguth, C. 2010 Climate response at the Paleocene-

   Eocene Thermal Maximum to greenhouse gas forcing - a model study with CCSM3. *J.

   Climate* **23**, 2562-2584.

22 Sewall, J. O., Sloan, L.C., Huber, M. & Wing, S. 2000 Climate sensitivity to changes in land

   surface characteristics. *Global Plan. Change* **26**, 445-465.

23 Zeebe, R. E., Zachos, J. C. & Dickens, G. R. 2009 Carbon dioxide forcing alone insufficient

   to explain Palaeocene-Eocene Thermal Maximum warming. *Nature Geosc.* **2**, 576-580.

24 Panchuk, K., Ridgwell, A. & Kump, L. R. 2008 Sedimentary response to Paleocene-Eocene

   Thermal Maximum carbon release: A model-data comparison. *Geology* **36**, 315-318.

25 Zachos, J. C., Dickens, G. R. & Zeebe, R. E. 2008 An early Cenozoic perspective on

   greenhouse warming and carbon-cycle dynamics. *Nature*, **451**, 279-283.

26 Renssen, H., Beets, C.J., Fichefet, T., Goosse, H. & Kroon, D. 2004 Modeling the climate

   response to a massive methane release from gas hydrates. Paleocean. **19**,

   (doi:10.1029/2003PA000968)

27 Ramanathan, V., Crutzen, P.J., Kiehl, J.T. & Rosenfeld, D. 2001 Aerosols, climate, and the

   hydrological cycle. *Science* **294**, 2119-2124.

28 Zachos, J.C., Schouten, S., Bohaty, S., Quattlebaum, T., Sluijs, A., Brinkhuis, H., Gibbs, S.J. & Bralower, T.J. 2006 Extreme warming of mid-latitude coastal ocean during the Paleocene-Eocene Thermal Maximum: Inferences from TEX_{86} and isotope data. *Geology*, **34**, 737-740.

29 Weijers, J. W. H., Schouten, S., Sluijs, A., Brinkhuis, H., Damste, J.S.S. 2007 Warm arctic continents during the Palaeocene-Eocene thermal maximum. *Earth Plan. Sci. Lett*. **261**, 230-238.

30 Sluijs, A., Bijl, P. K., Schouten, S., Röhl, U., Reichart, G.-J. & Brinkhuis, H. 2011 Southern ocean warming, sea level, and hydrological change during the Paleocence-Eocene thermal maximum. *Clim. Past* **7**, 47-61 (doi:10.5194/cp-7-47-2011).

31 Bilj, P.K., Schouten, S., Sluijs, A., Reichart, G-J., Zachos, J.C. & Brinkhuis, H. 2009 Early Paleogene temperature evolution of the Southwest Pacific ocean. *Nature*, **461**, 776-779.

32 Dunkley Jones, T. D., Ridgwell, A., Lunt, D.J., Maslin, M.A., Schmidt, D.N. & Valdes, P.J. 2010 A Paleogene perspective on climate sensitivity and methane hydrate instability. *Phil. Trans. R. Soc. A*. **368**, 2395-2415.

33 Lunt, D.J., Valdes, P.J., Dunkley Jones, T., Ridgwell, A., Haywood, A.M., Schmidt, D.N., Marsh, R. & Maslin, M. 2010 CO2-driven ocean circulation changes as an amplifier of Paleocene-Eocene thermal maximum hydrate destabilization. *Geology* **38**, 875-878 (doi: 10.1130/G31184.1).

34 Cope, J.T. & Winguth, A. 2011 On the sensitivity of ocean circulation to arctic freshwater input during the Paleocene/Eocene Thermal Maximum. *Paleog. Paleoclim. Paleoc*. **306**, 82-94 (doi:10.1016/j.paleo.2011.03.032).

35 Bice, K.L. & Marotzke, J. 2001 Could changing ocean circulation have destabilized methane hydrate at the Paleocene/Eocene boundary? *Paleoceanog.*, **16**, doi:10.1029/2001PA000678.

36 Miller, K.G, Janecek, T.R., Katz, M.E. & Keil, D.J. 1987 Abyssal circulation and benthic foraminiferal changes near the Paleocene/Eocene boundary. *Paleoceanog.*, **2**, 741-761.

37 Thomas, D.J., Bralower, T.J. & Jones, C.E. 2003 Neodymium isotopic reconstruction of late Paleocene-early Eocene thermohaline circulation. *Earth and Planetary Sci. Lett*. **209**, 309-322.

38 Nunes, F. & Norris, R. D. 2006 Abrupt reversal in ocean overturning during the Paleocene/Eocene warm period. *Nature* **439**, 60-63.

39 Huber, M. & Sloan, L. C. 2001 Heat transport, deep waters, and thermal gradients; coupled simulation of an Eocene greenhouse climate. *Geophys. Res. Lett*. **28**, 3481-3484.

40 Wing, S. L., Harrington, G.J., Smith, F.A., Bloch, J.I., Boyer, D.M. & Freeman, K.H. 2005 Transient floral change and rapid global warming at the Paleocene-Eocene boundary. *Science* **310**, 993-996.

41 Greenwood, D. R., Basinger, J.F. & Smith, R.Y. 2010 How wet was the Arctic Eocene rain forest? Estimates of precipitation from Paleogen Arctic macrofloras. *Geology* **38**, 15-18.

42 Hansen, J., Sato, M., Kharecha, P., Beerling, D., R. Berner, Masson-Delmotte, V., Pagani, M., Raymo, M., Royer, D.L. & Zachos, J.C. 2008 Target atmospheric CO_2: Where should humanity aim? *Open Atmos. Sci. J.*, **2**, 217-231, (doi:10.2174/1874282300802010217)

43 Lunt, D. J., Haywood, A. M., Schmidt, G. A., Salzmann, U., Valdes, P. J. & Dowsett, H. J. 2010 Earth system sensitivity inferred from Pliocene modelling and data. Nature Geosc. 3, 60 – 64 (doi:10.1038/ngeo706).

44 Haywood, A. M., Ridgwell, A., Lunt, D. J., Hill, D. J., Pound, M. J., Dowsett, H. J., Dolan, A. M., Francis, J.E. & Williams, M. 2011 Are there pre-Quaternary geological analogues for a

future greenhouse warming? *Phil. Trans. Roy. Soc. A* **369**, 933-956

(doi:10.1098/rsta.2010.0317).

45 Hansen, J., Sato, M., Nazarenko, L., Ruedy, R. , Lacis, A., Koch, D., Tegen, I. , Hall, T. ,

Shindell, D., Santer, B., Stone, P., Novakov, T., Thomason, L., Wang, R., Wang, Y., Jacob,

D., Hollandsworth, S., Bishop, L., Logan, J., Thompson, A., Stolarski, R., Lean, J., Willson,

R., Levitus, S., Antonov, J., Rayner, N., Parker, D. & Christy, J. 2002 Climate forcings in

Goddard Institute for Space Studies SI2000 simulations, *J. Geophys. Res.*, **107(D18)**, 4347,

(doi:10.1029/2001JD001143).

46 Sloan, L. C., Walker, J.C.G., Moore Jr., T.C., Rea, D.K. & Zachos, J.C. 1992 Possible

methane-induced polar warming in the early Eocene. *Nature* **357**, 320-322.

47 Kiendler-Scharr, A., Wildt, J., Dal Maso, M., Hohaus, T., Kleist, E., Mentel, T.F., Tilman, R.,

Uerlings, R., Schurr, U. & Wahner, A. 2009 New particle formation in forests inhibited by

isoprene emissions. *Nature* **461**, 381-384.

48 Spicer, R. A. & Chapman, J. L. 1990 Climate change and the evolution of high-latitude

terrestrial vegetation and floras. *Trends in Eco. & Evo*. **5**, 279-284.

49 Head, J. J., Bloch, J. I., Hastings, A. K., Bourque, J. R., Cadena, E. A., Herrera, F. A., David

Polly, P. & Jaramillo, C. A. 2009 Giant boid snake from the Palaeleocene neotropics reveals

hotter past equatorial temperatures. Nature 457, 715-717 (doi:10.1038/nature07671).

50 Tripati, A. & Elderfield, H. 2005 Deep-sea temperature and circulation changes at the

Paleocene-Eocene Thermal Maximum. *Science*, **308**, 1894-1898.

Figure Captions

Figure 1. Zonal mean change in: a) PETM annual surface-air temperature (°C) due to changes in

CO_2 from 280 ppmv to 2250 ppmv (--------), changes in CH_4 from 760 ppbv to 16 ppmv (-- -- -- -

-) and changes in cloud cloud properties (_____), b) annual surface-air temperature normalized

by respective global mean change in surface air temperature due to changes in CO_2 from 280

ppmv to 2250 ppmv (--------), changes in CH_4 from 760 ppbv to 16 ppmv (-- -- -- --) and changes

in cloud cloud properties (_____).Normalized value = $([T_s]_{exp}-[T_s]_{control})/<T_s>_{control}$, where [ ]

indicates zonal mean and < > indicates global mean.

Figure 2. Zonal annual mean sea surface temperatures (°C) from the modern (_____), PETM

(_____) and PRE-PETM (_____)CCSM3 simulations.

Figure 3. Geographic distribution simulated: a) PETM sea surface temperatures (°C) and, b)

change in sea surface temperature (°C) from PRE-PETM to PETM climate. Numbers in boxes

are observed range in temperature changes [32].

Figure 4. PETM simulated a) sea surface salinity (practical salinity units), b) evaporation minus

precipitation (mm/day), c) surface runoff (mm/day).

Figure 5. Simulated maximum mixed layer depths (m) for a) January PRE-PETM, b) February

PRE-PETM, c) July PRE-PETM, d) August PRE-PETM, e) January PETM, f) February PETM,

g) July PETM, h) August PETM,

Figure 6. Simulated 1000 m potential temperature (°C) and ocean currents (cm/s) for a) PETM

and b) PRE-PETM simulations.

Figure 7. PETM simulated 100 meter vertical velocity to denote regions of upwelling (positive)

and 100 m surface ocean currents.

Figure 8. Zonal annual mean of ocean poleward heat transport (PW) for the modern (_____),

PRE-PETM (--------) and PETM (- - - - - -) simulations.

Figure 9. Zonal annual mean ocean potential temperature (°C) for simulated : a) PETM, b) PRE-

PETM and c) Present climate simulations.

Figure 10. Vertical profiles of potential temperature (°C) for December-January-February

average: a) tropical, b) northern high latitudes, and for June-July-August average c) tropical, d)

southern high latitudes. PETM case is solid line (_____), PRE-PETM case is dashed line (------).

Figure 11. Simulated annual mean: a) PETM surface-air temperature (°C) and b) change in

surface-air temperature (°C) from PRE-PETM to PETM climate.

Figure 12. Simulated cold month mean (°C): a) PETM and b) PRE-PETM.

Figure 13. Comparison of simulated terrestrial surface-air temperatures (°C) with the Huber and

Caballero [12] proxy database for the: a) PETM and b) PRE-PETM climates.

Figure 14. Difference in annual mean PETM surface temperature (°C) between simulation

assuming a continental cloud drop density of 400 cm^{-3} and drop effective radius of 10 microns

with a simulation assuming a continental cloud drop density of 50 cm^{-3} and effective radius of 17

microns.

Figure 15. Percent change in terrestrial precipitation between the PETM and PRE-PETM climate

simulations.

Submitted to Phil. Trans. R. Soc. A - Issue

Page 32 of 47

Table 1

Comparison of modeled PETM surface temperatures (°C) for various locations including marine and terrestrial sites. Data are from Table 1 in [28-31], [49]. Numbers in parentheses ( ) are mean annual model values and values in square brackets [ ] are summer model values. * denotes terrestrial reconstructions.

Paleo latitude	Surface Temperature (°C)
75 °N (Arctic)	25 (17) [28]
47 °N (Big Horn, WY)*	20-26 (25) [40]
~36 °N (NJ Coast)	33 (32) [37]
~6 °N (Columbia)*	38-40 (38) [37]
55 °S (New Zealand)	33 (23) [28]
65 °S	25 (23) [28]

Table 2

Comparison of modeled PETM ocean temperatures (°C) with reconstructions for three locations and ocean depths (m). Data are from [50].

Paleo latitude	Depth (m)	Temperature (°C)
~30°S (S. Atlantic)	~3400	14-15 (15)
~10-15 °N (Pacific)	~2400	13-21 (15)
~2 °N (Eq. Pacific)	~1300	13-17 (17)
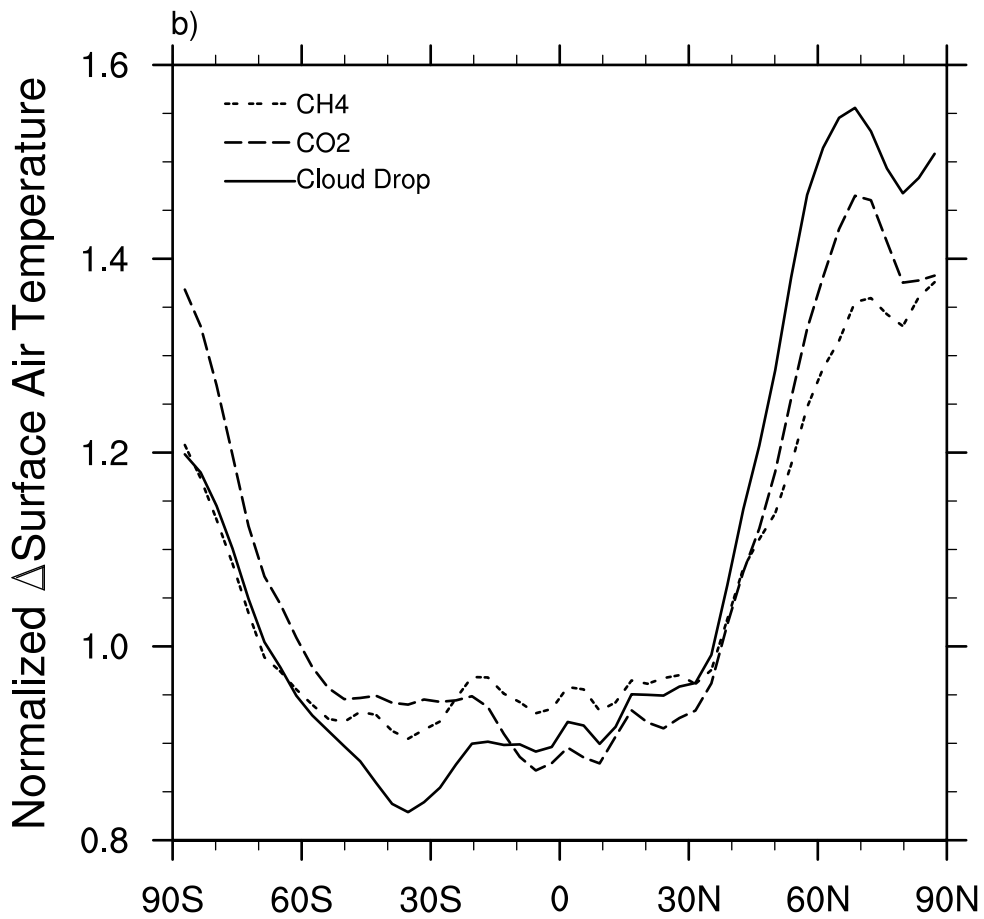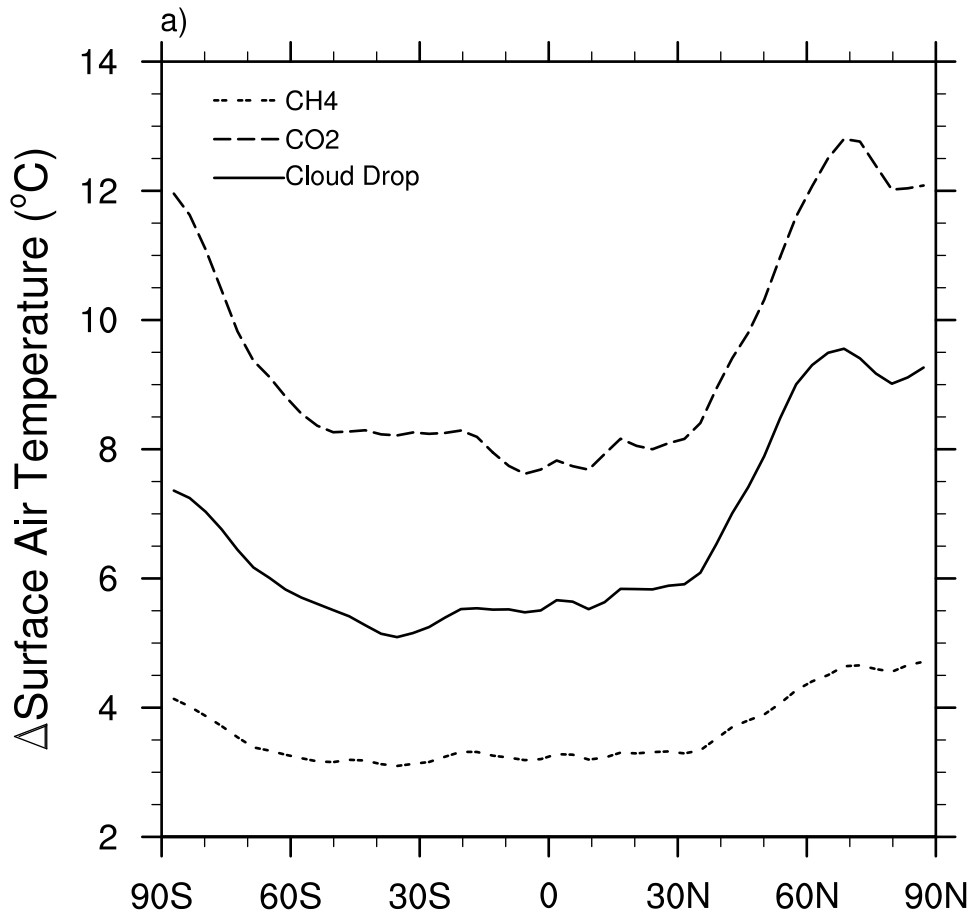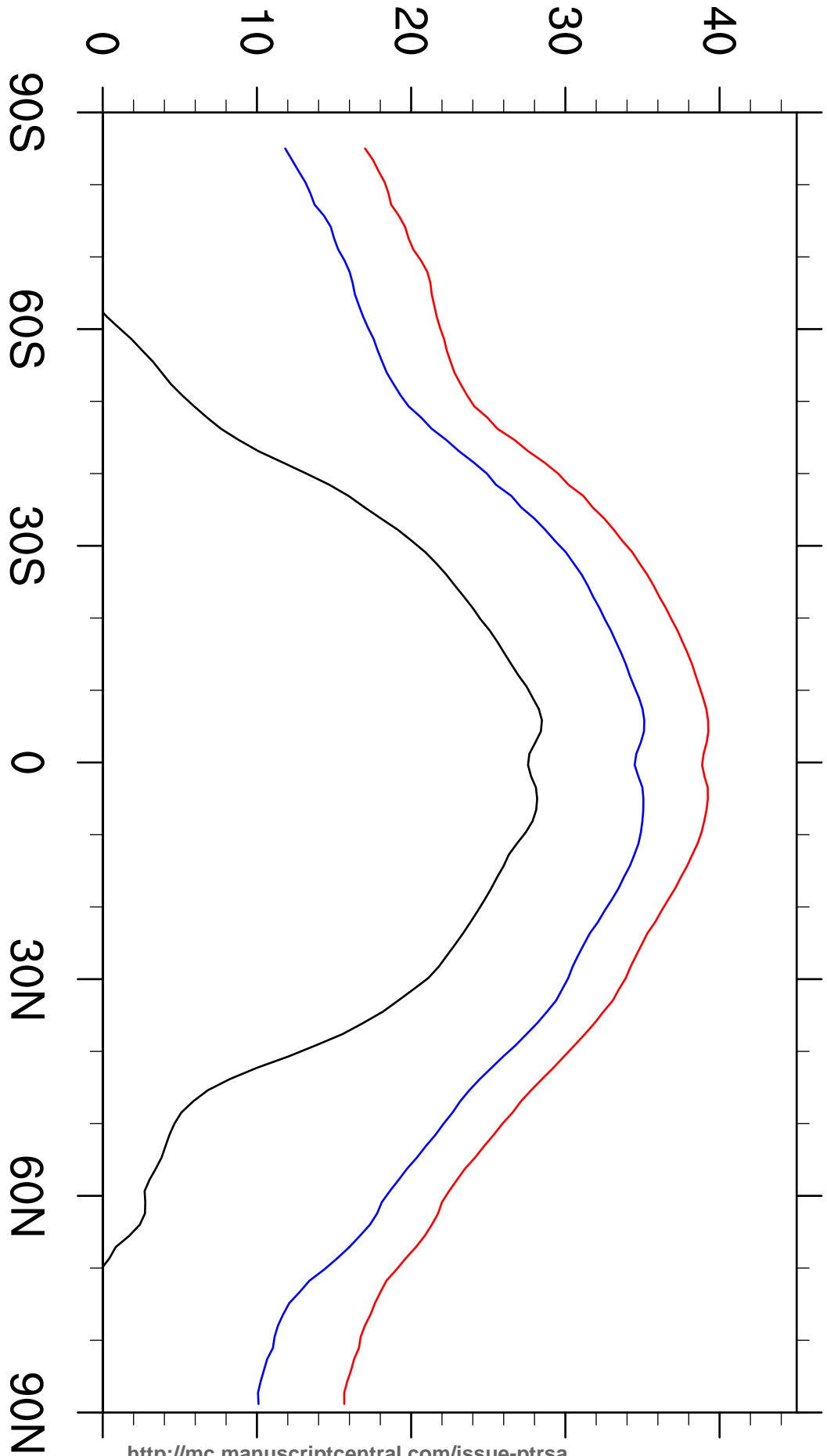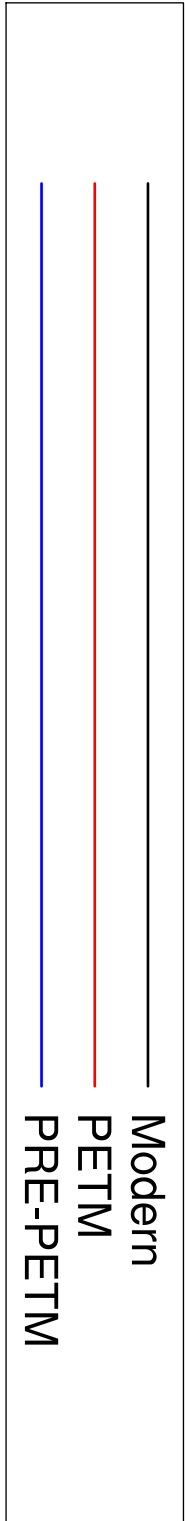
Page 33 of 47

Submitted to Phil. Trans. R. Soc. A - Issue

Page 35 of 47

Submitted to Phil. Trans. R. Soc. A - Issue

1
2
3
4
5
6
7
8
9
10
11
12
13
14
15
16
17
18
19
20
21
22
23
24
25
26
27
28
29
30
31
32
33
34
35
36
37
38
39
40
41
42
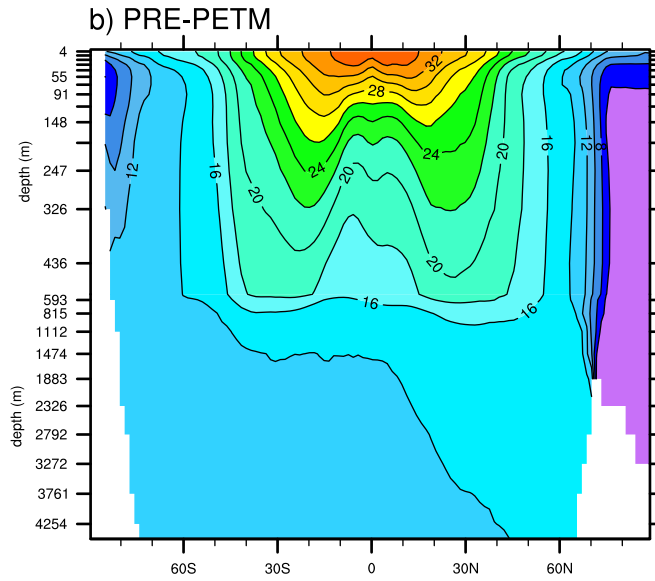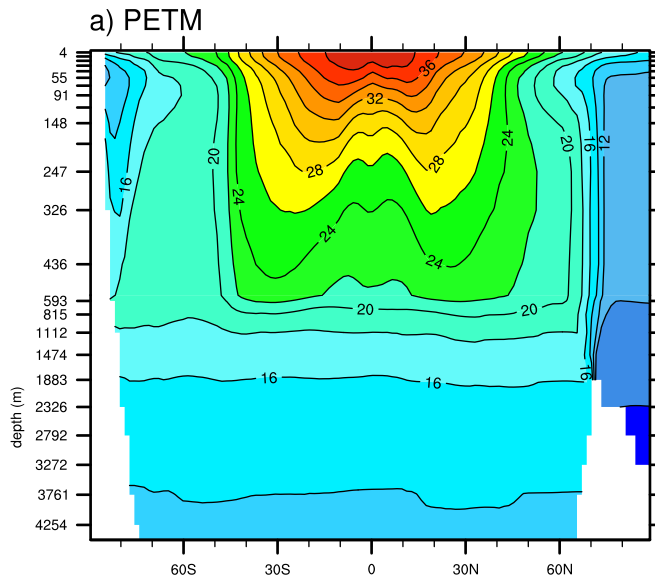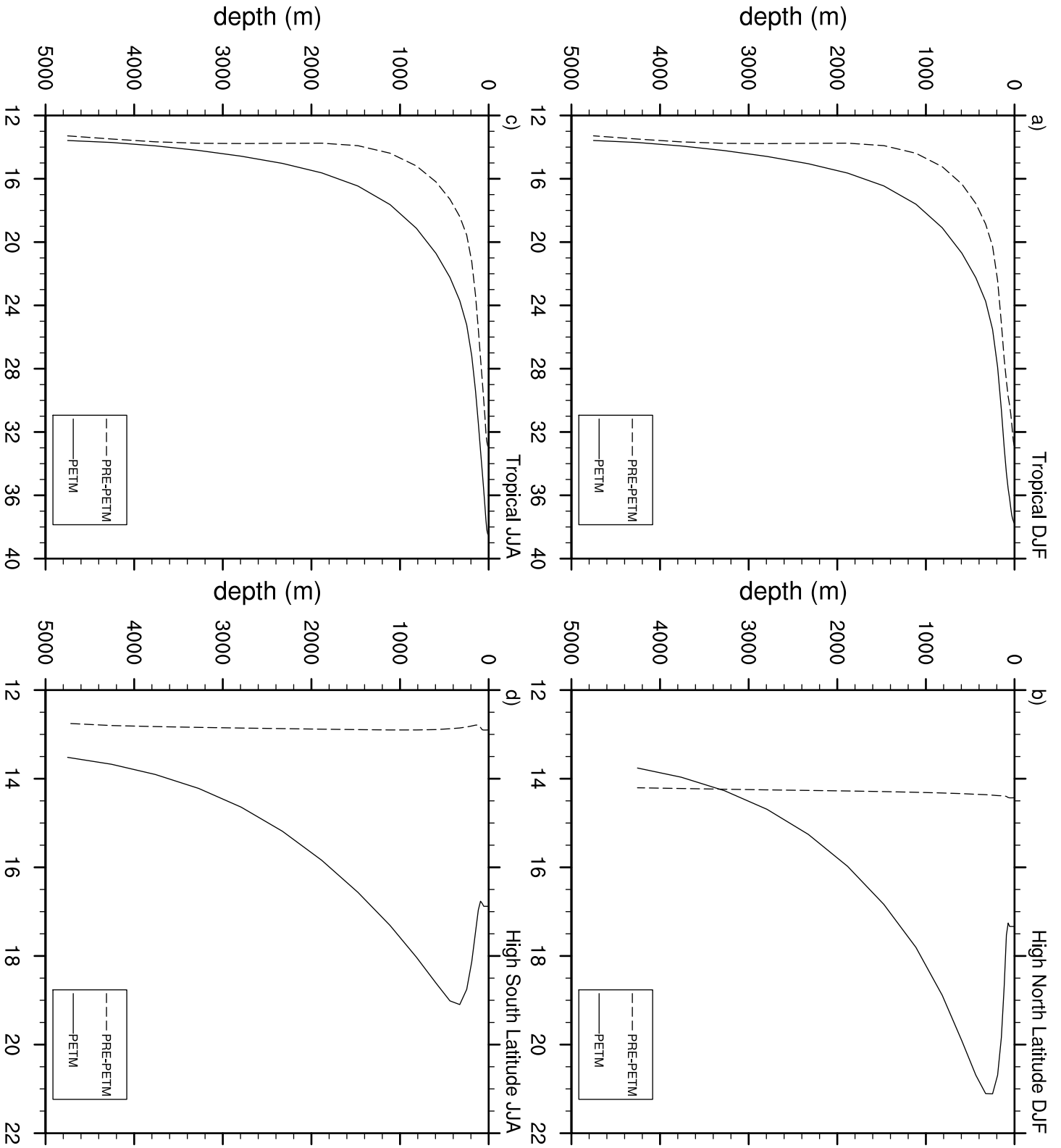43
44
45
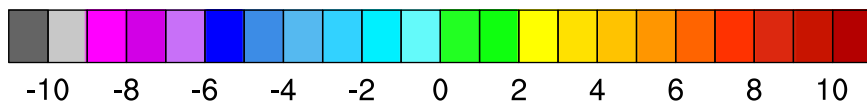46
47
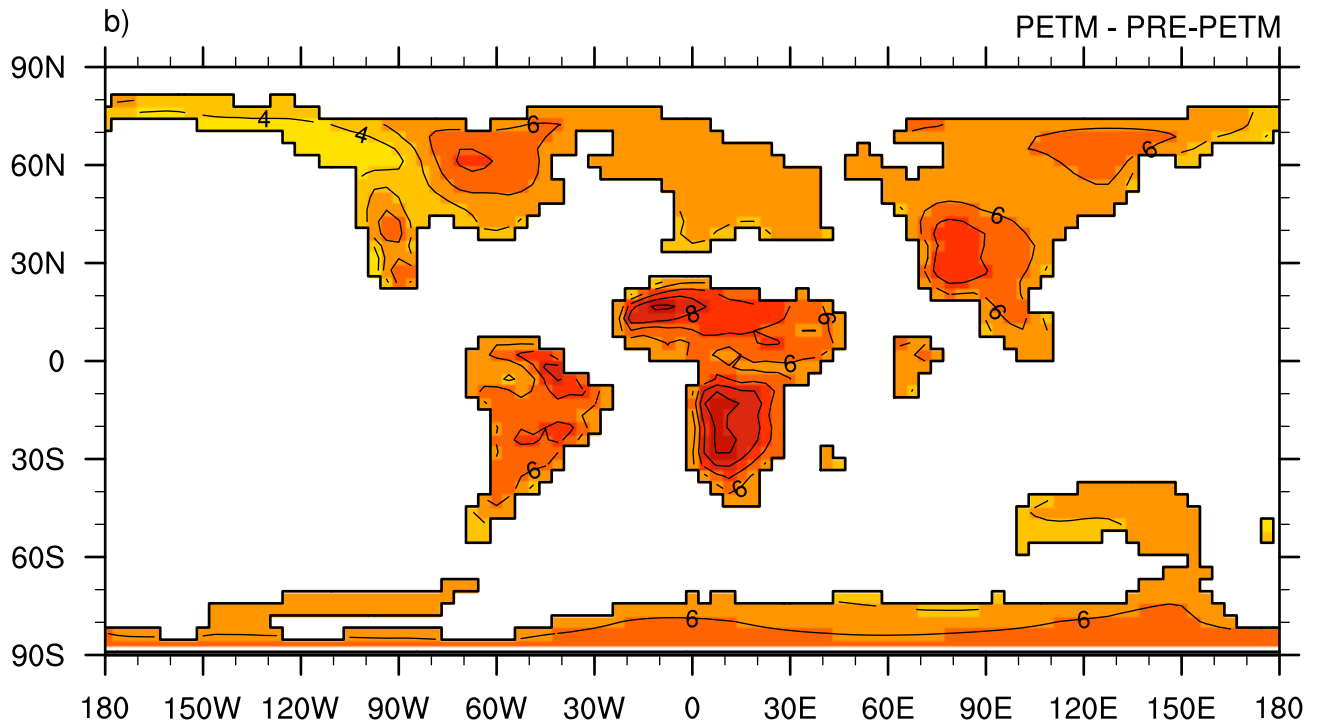48
49
50
51
52
53
54
55
56
57
58
59
60

Submitted to Phil. Trans. R. Soc. A - Issue

Page 36 of 47

SSS (psu)

a)

E-P (mm/day)

b)

Runoff Flux (mm/day)

c)

Page 37 of 47

Submitted to Phil. Trans. R. Soc. A - Issue

1
2
3
4
5
6
7
8
9
10
11
12
13
14
15
16
17
18
19
20
21
22
23
24
25
26
27
28
29
30
31
32
33
34
35
36
37
38
39
40
41
42
43
44
45
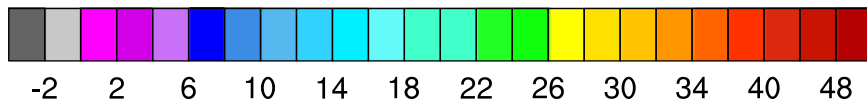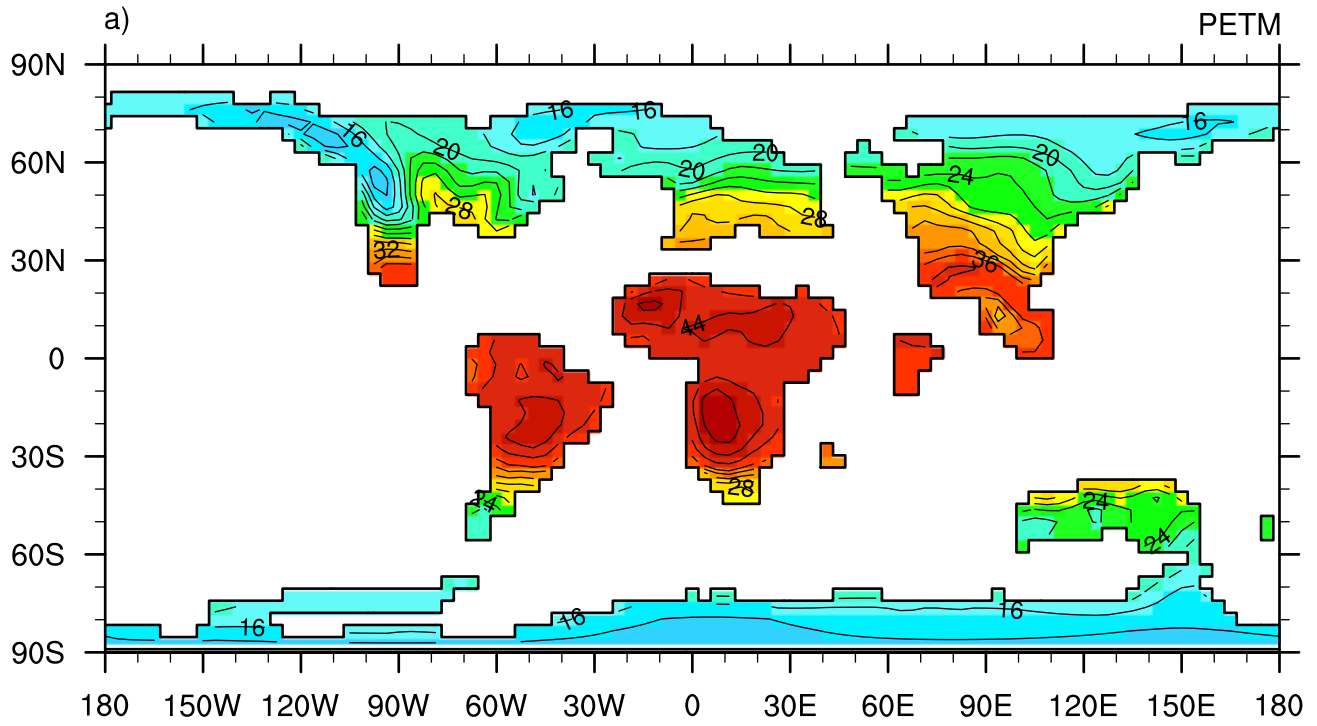46
47
48
49
50
51
52
53
54
55
56
57
58
59
60

Mixed Layer Depth (m)

Submitted to Phil. Trans. R. Soc. A - Issue

Page 38 of 47
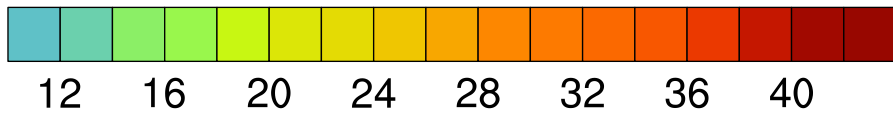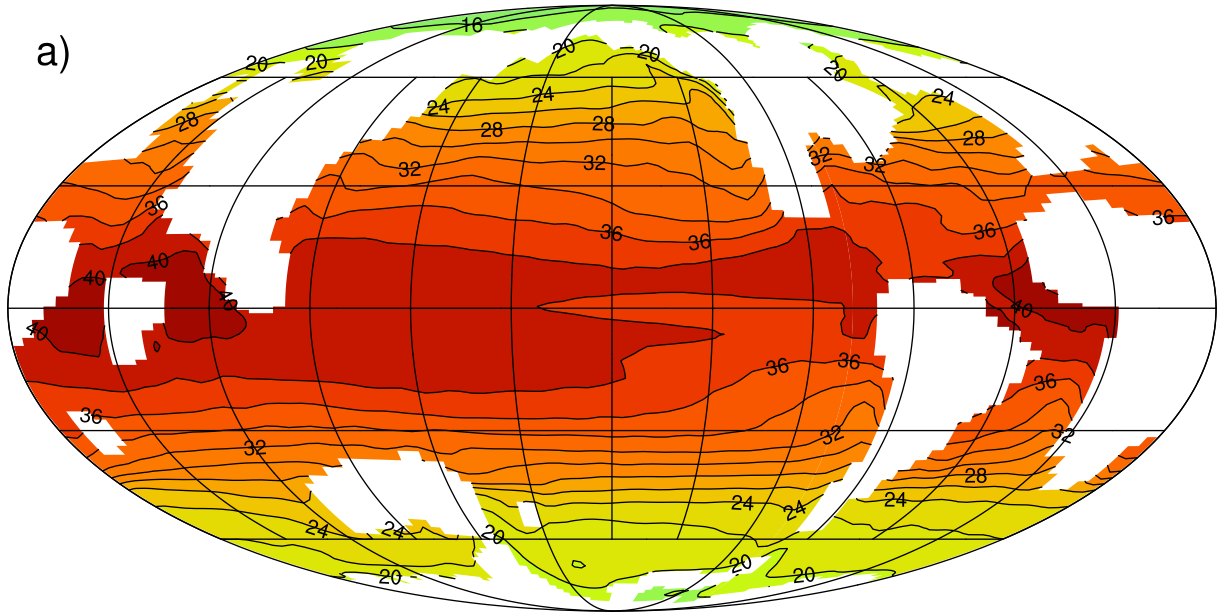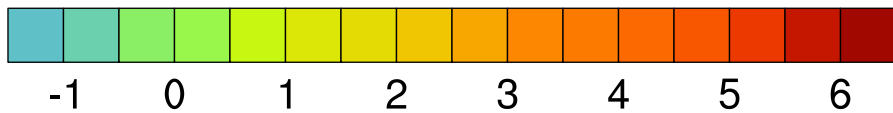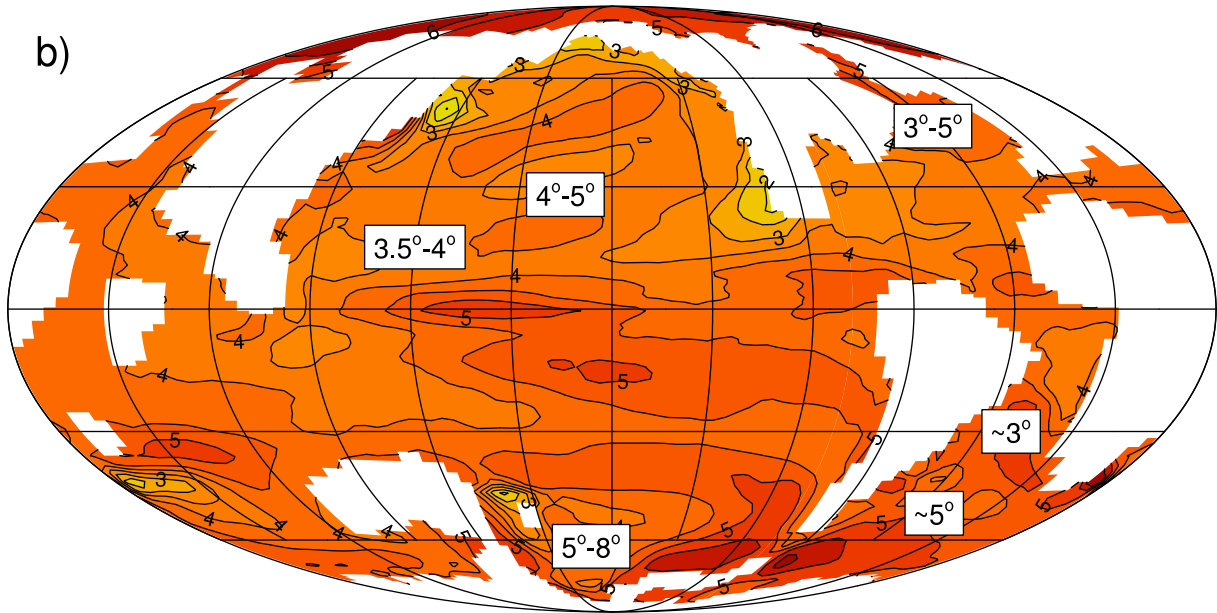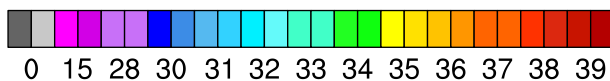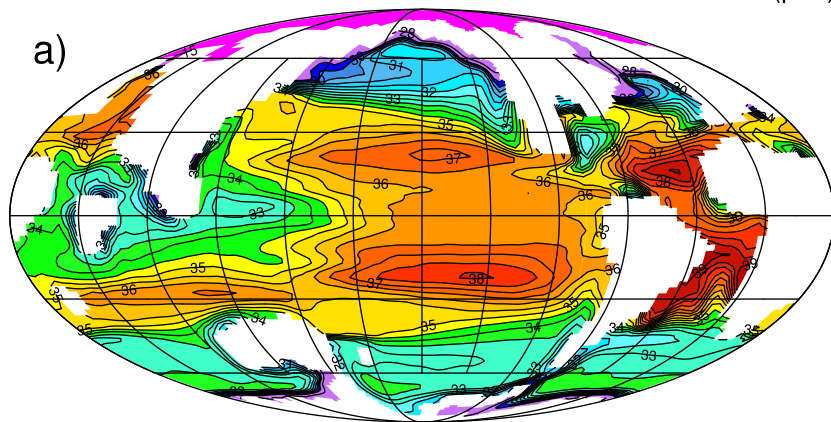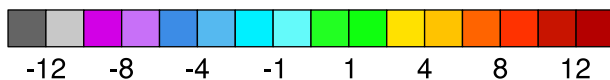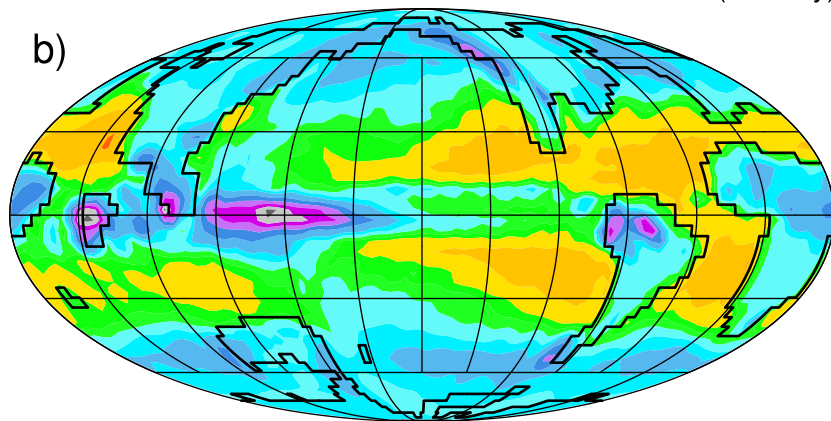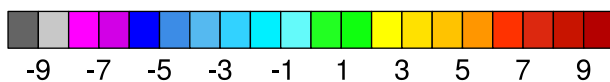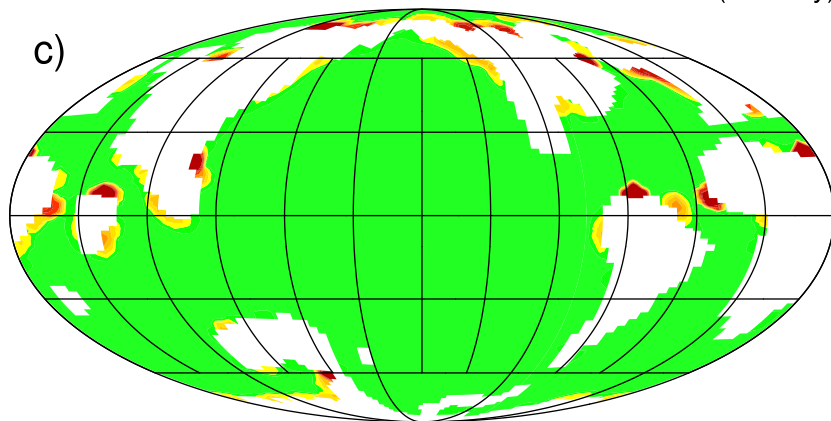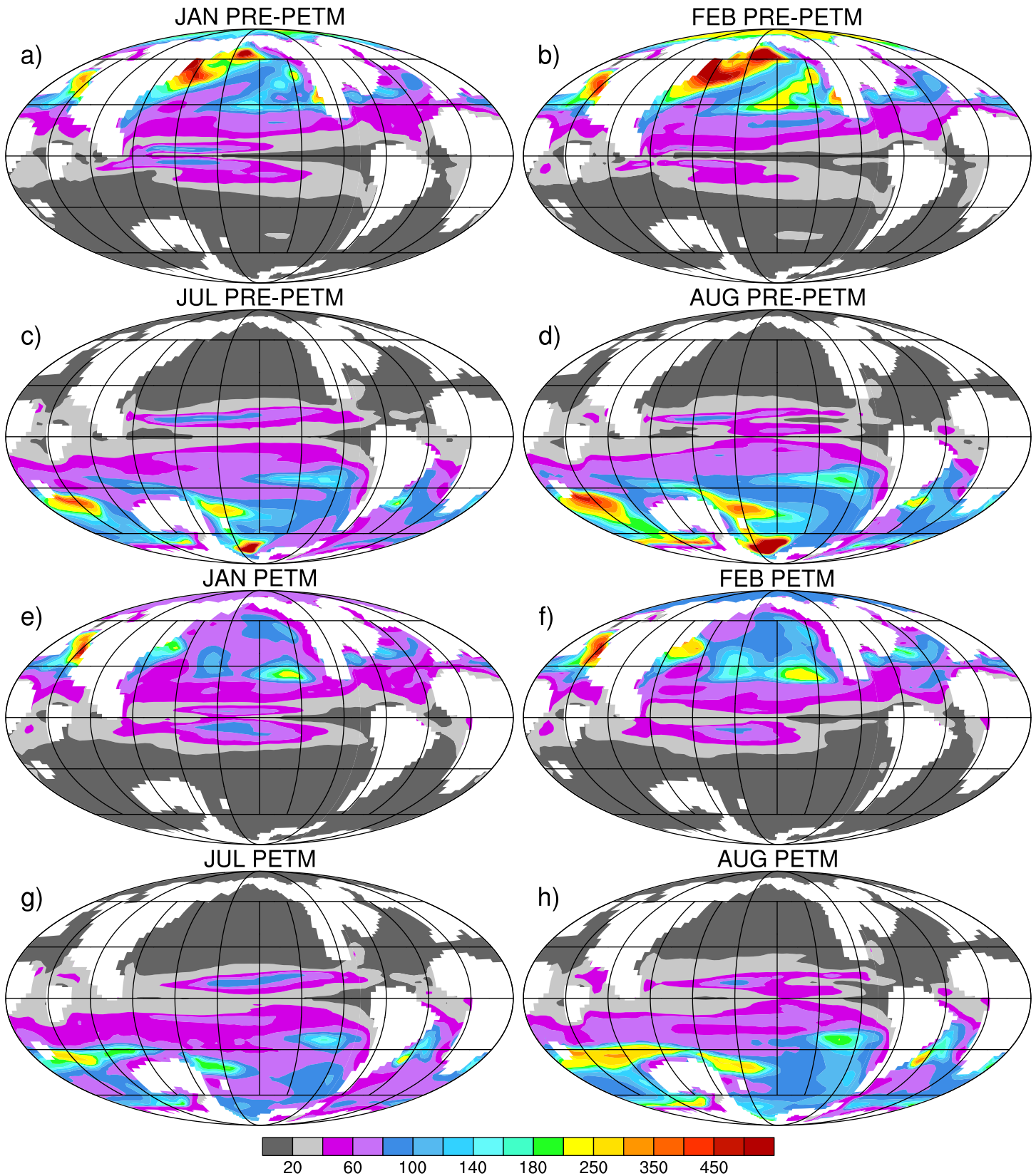
1000m Potential Temperature (°C) and Ocean Currents (cm/s)
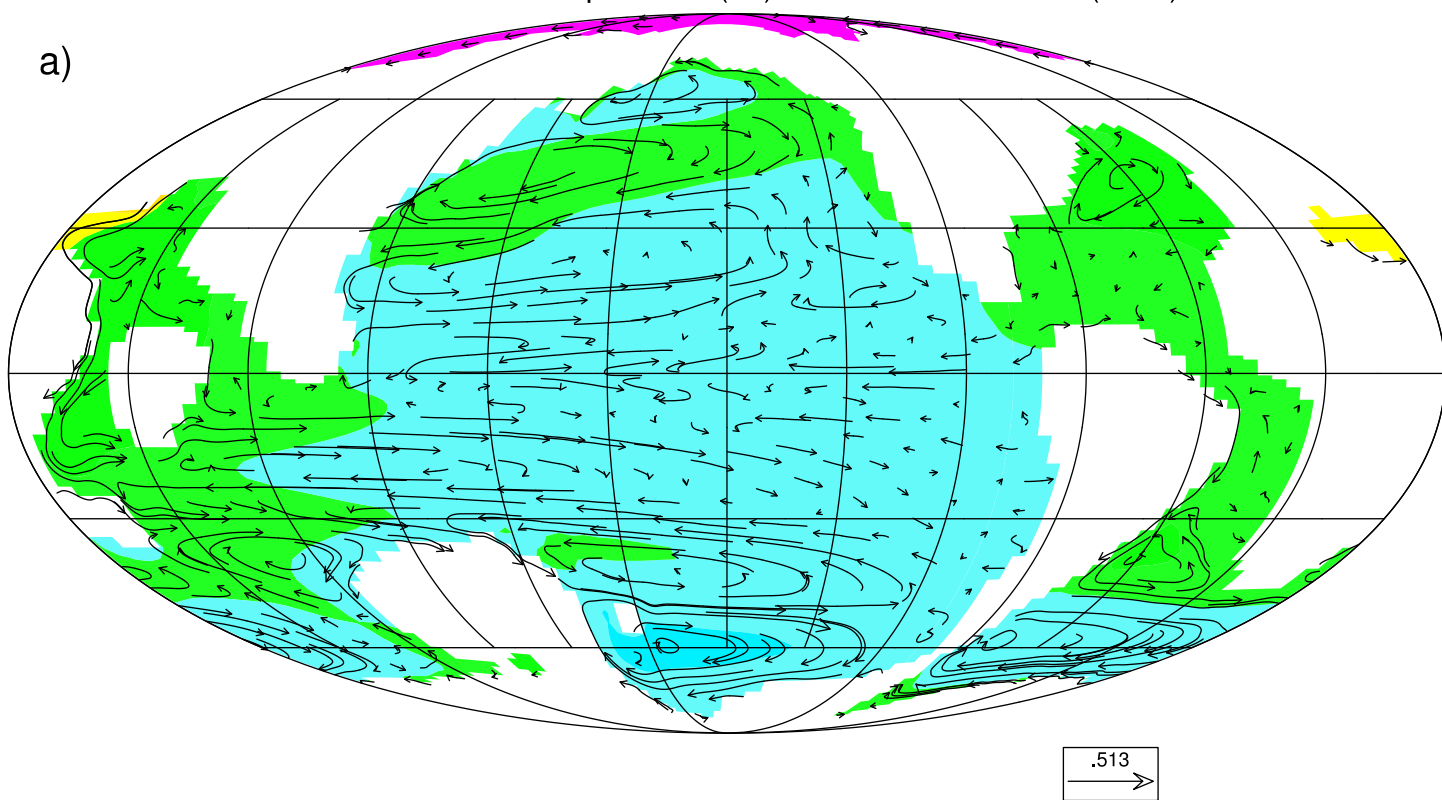
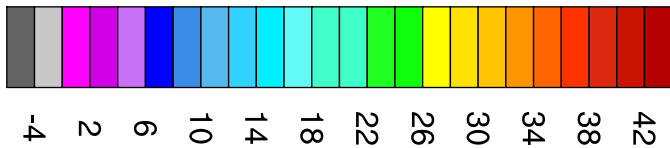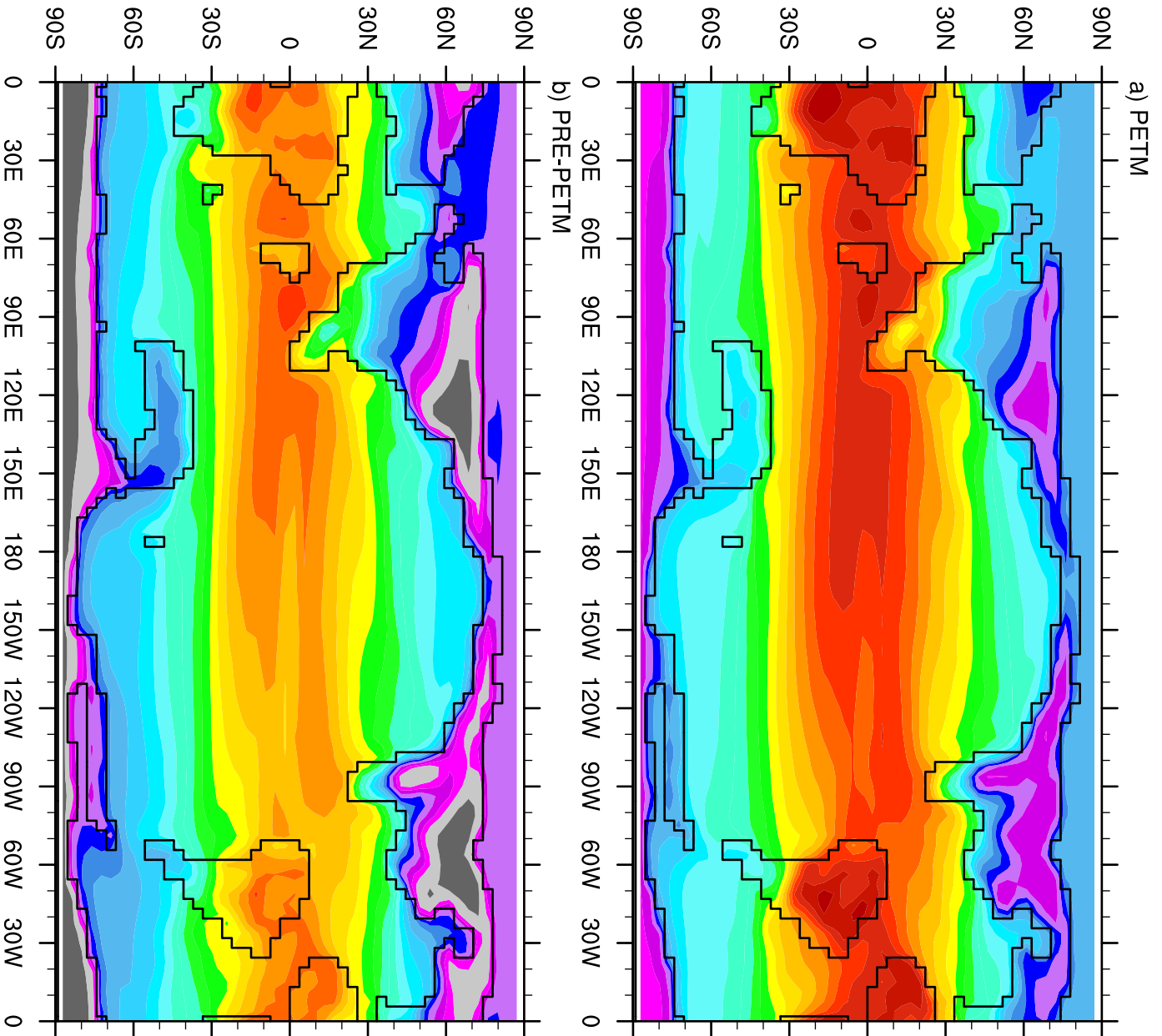1000m Potential Temperature (°C) and Ocean Currents (cm/s)
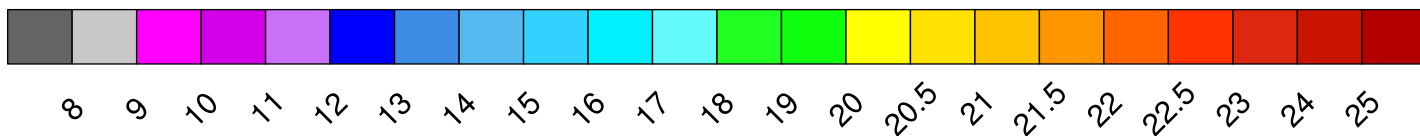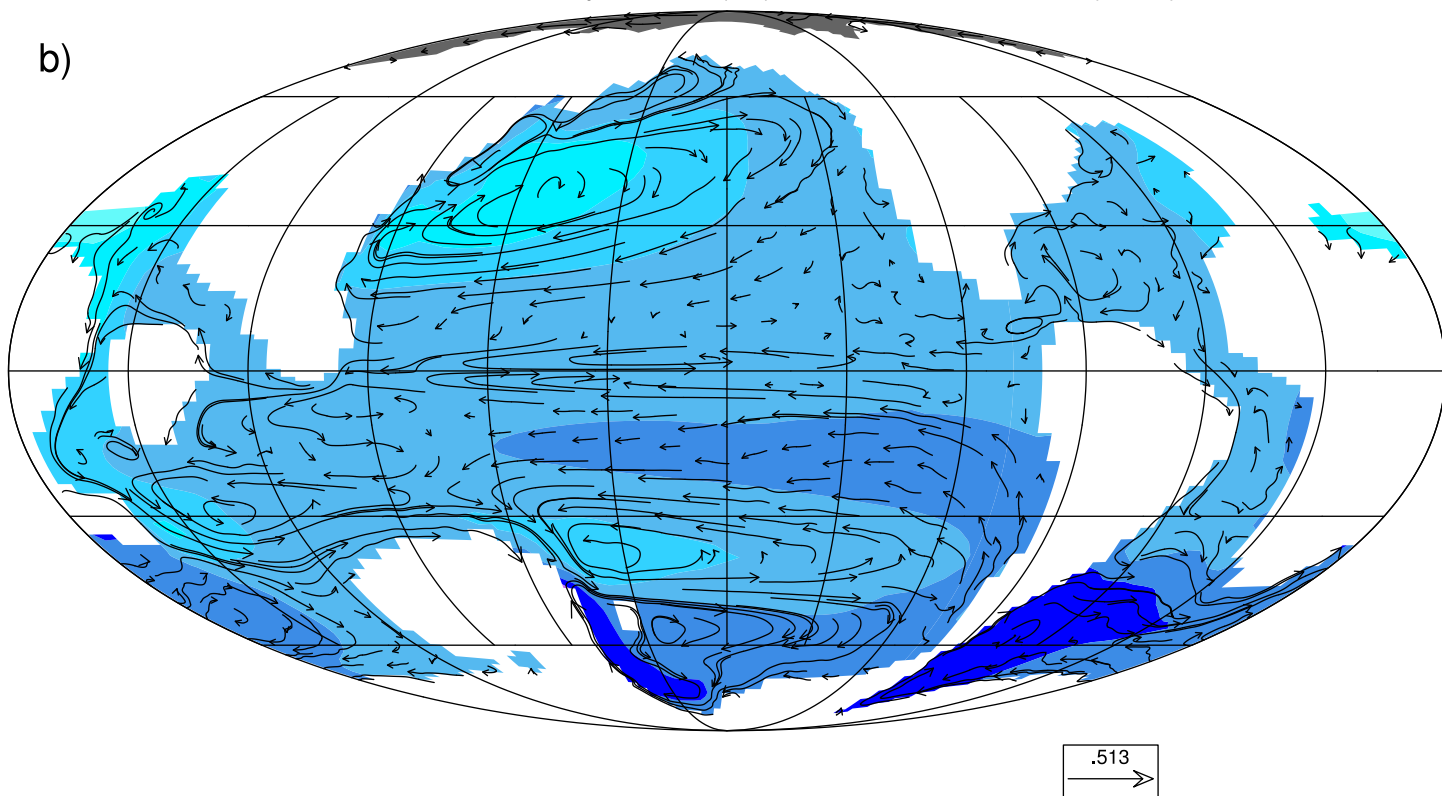
1
2
3
4
5
6
7
8
9
10
11
12
13
14
15
16
17
18
19
20
21
22
23
24
25
26
27
28
29
30
31
32
33
34
35
36
37
38
39
40
41
42
43
44
45
46
47
48
49
50
51
52
53
54
55
56
57
58
59
60
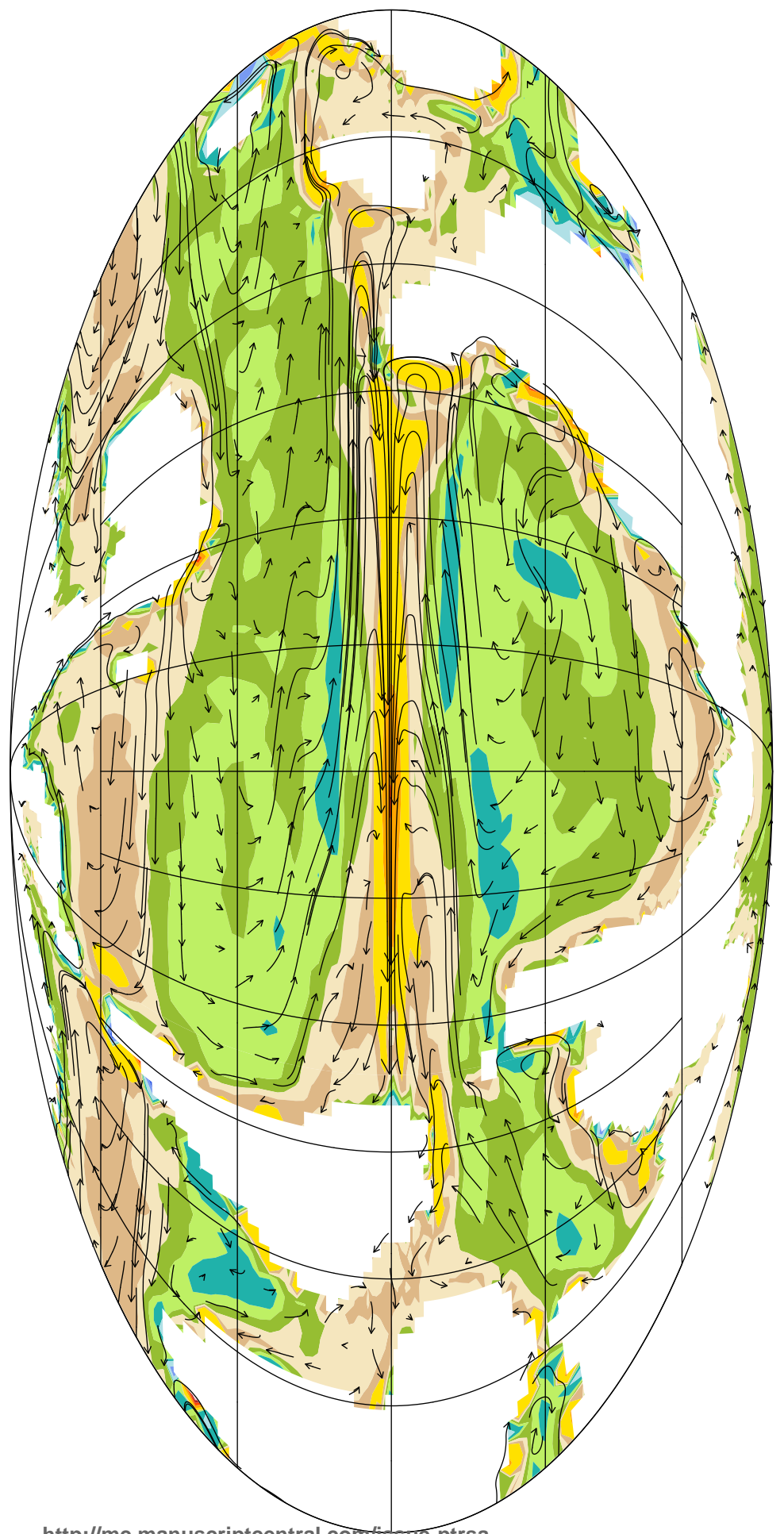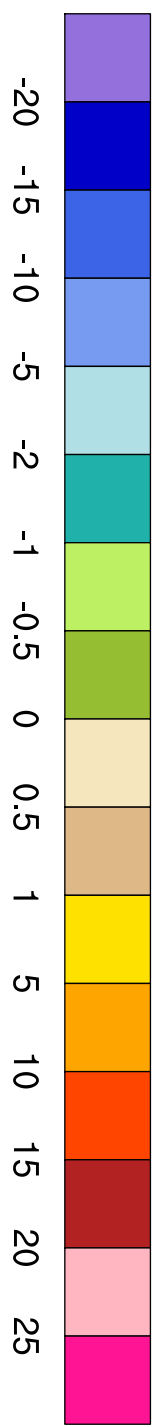
100m WVEL (10^{-4}x cm/s) and 100m Ocean Currents

Pw

Northward Heat Transport - Annual Mean
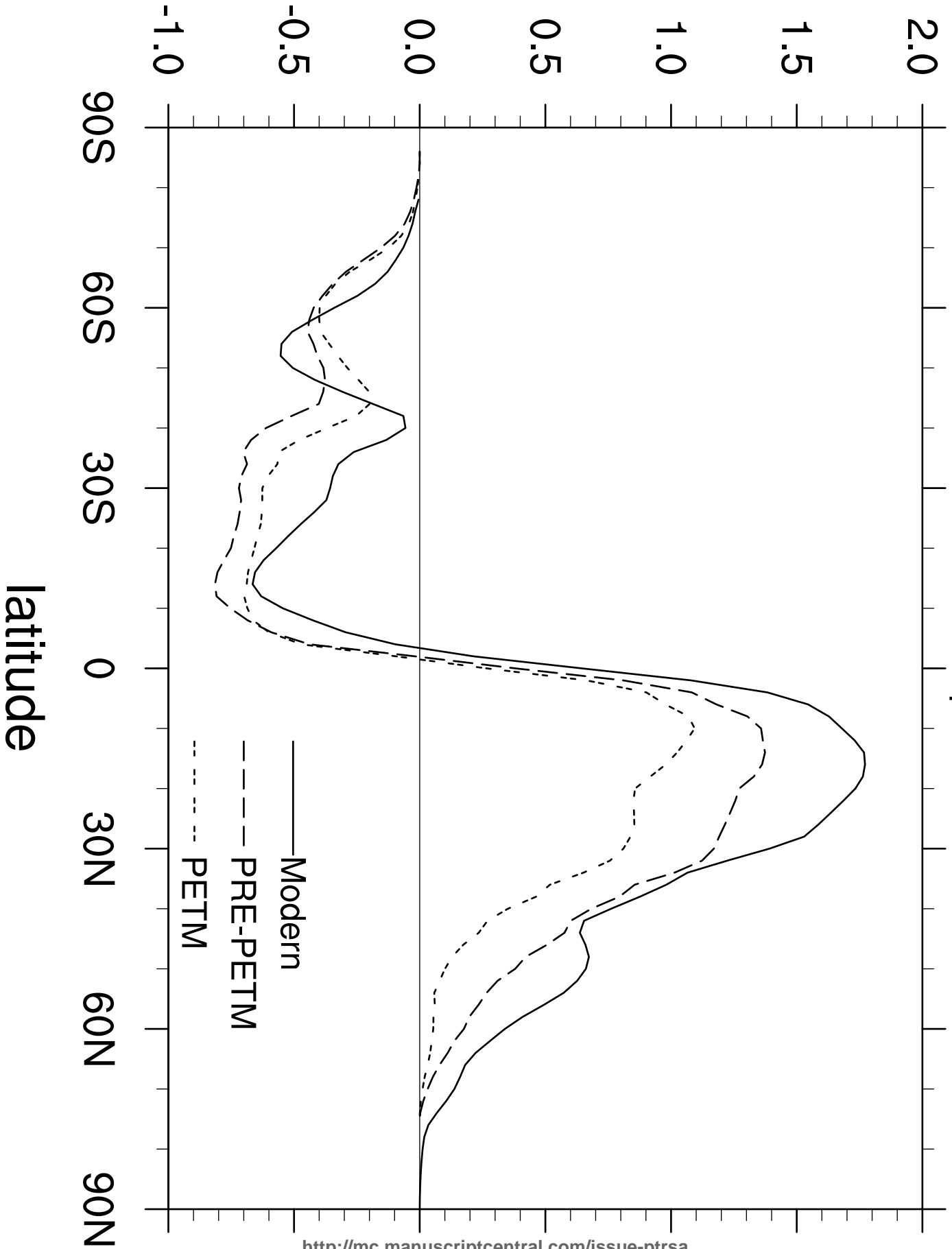
latitude

Modern
PRE-PETM
PETM

Page 41 of 47

Submitted to Phil. Trans. R. Soc. A - Issue

1
2
3
4
5
6
7
8
9
10
11
12
13
14
15
16
17
18
19
20
21
22
23
24
25
26
27
28
29
30
31
32
33
34
35
36
37
38
39
40
41
42
43
44
45
46
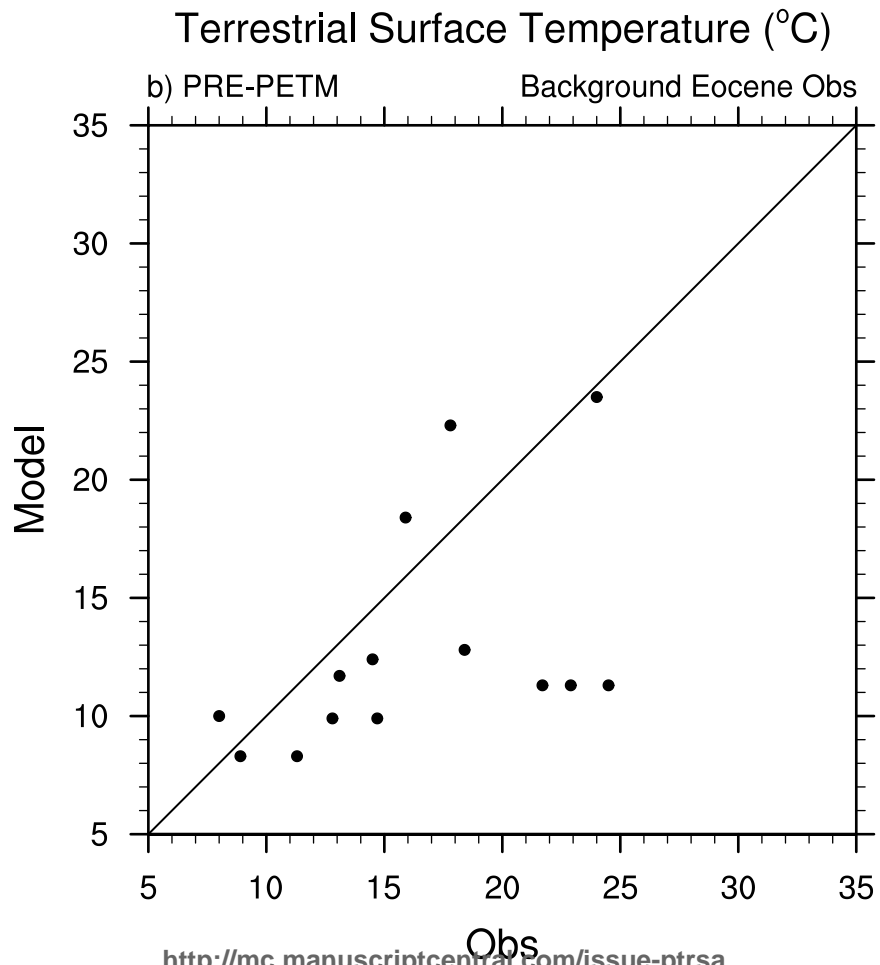47
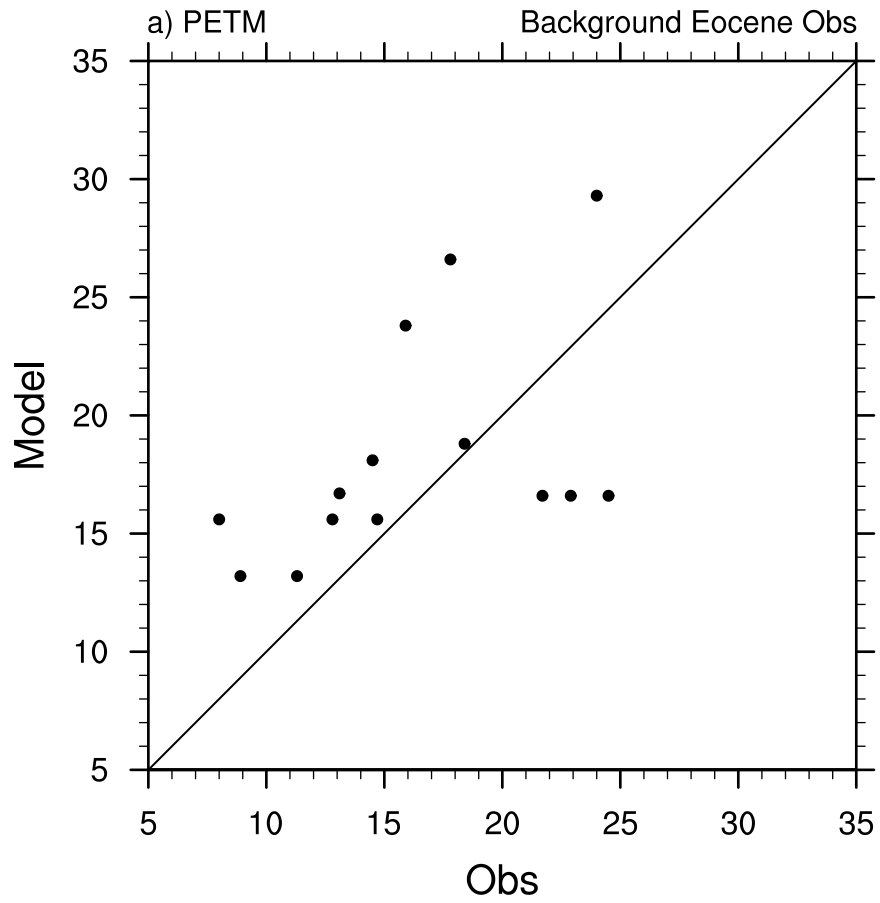48
49
50
51
52
53
54
55
56
57
58
59
60

Potential Temperature (°C)

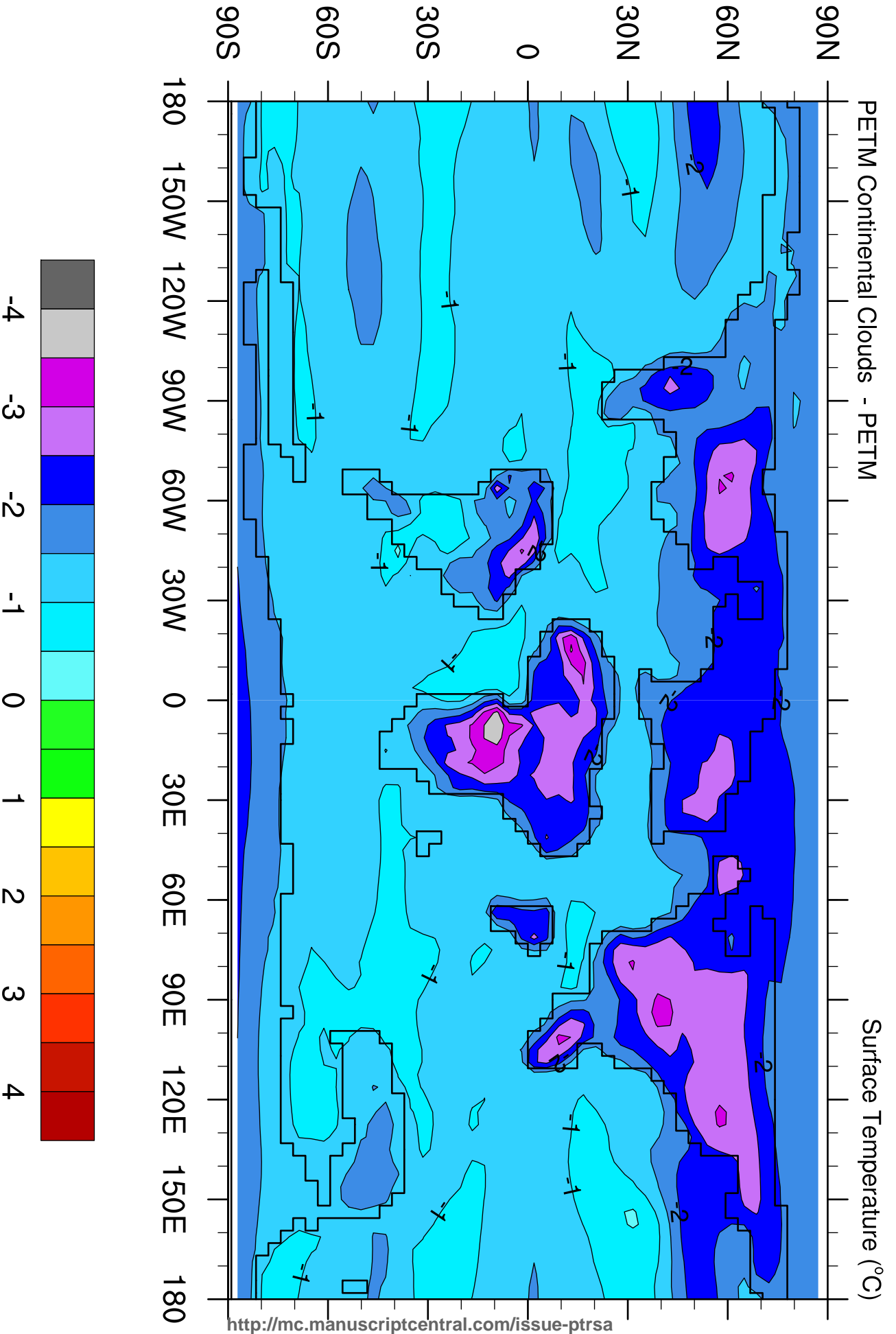Submitted to Phil. Trans. R. Soc. A - Issue

Page 42 of 47

Page 43 of 47

Submitted to Phil. Trans. R. Soc. A - Issue

Surface Air Temperature (^{o}C)

Submitted to Phil. Trans. R. Soc. A - Issue

Page 44 of 47
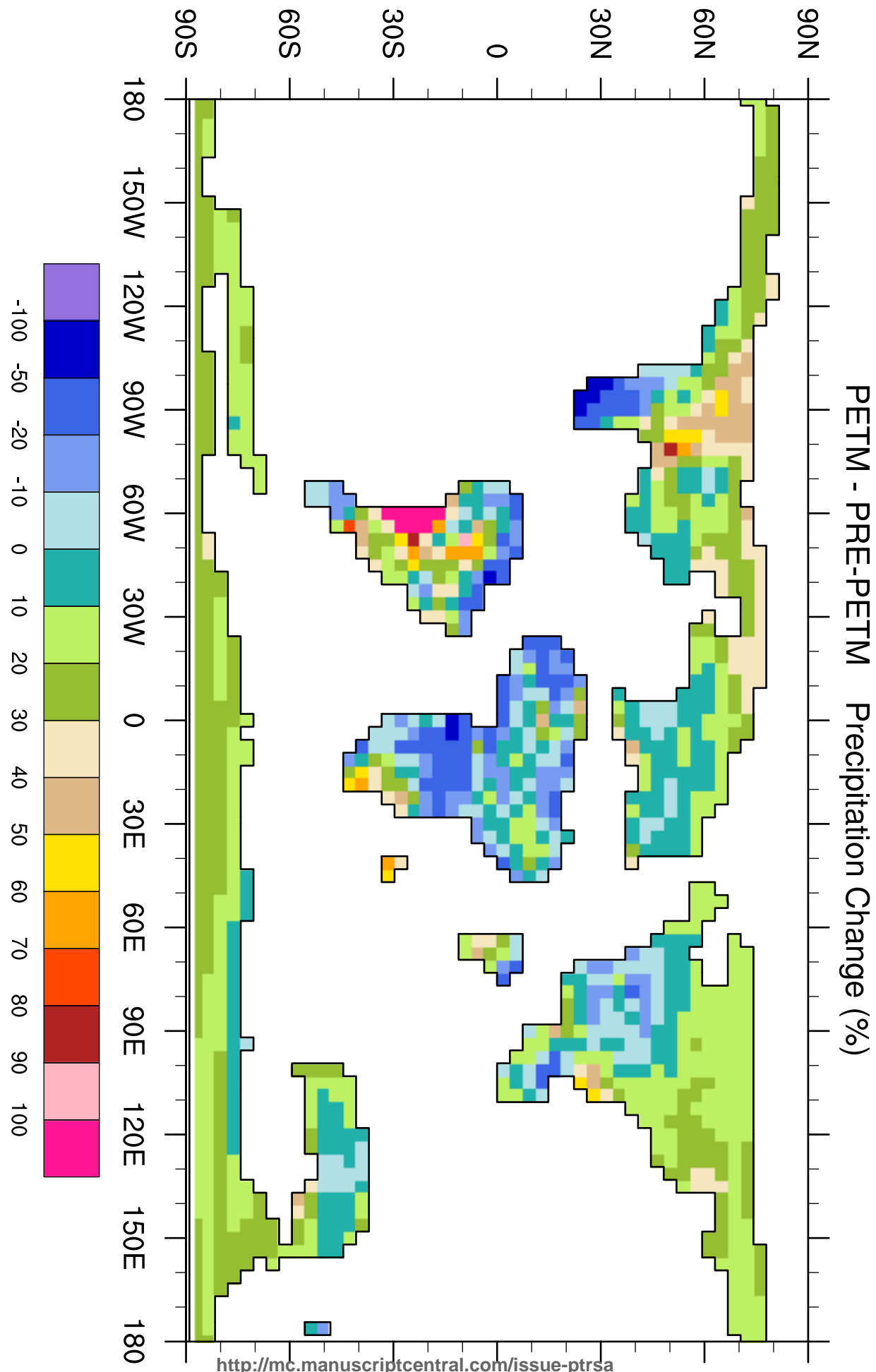
1
2
3
4
5
6
7
8
9
10
11
12
13
14
15
16
17
18
19
20
21
22
23
24
25
26
27
28
29
30
31
32
33
34
35
36
37
38
39
40
41
42
43
44
45
46
47
48
49
50
51
52
53
54
55
56
57
58
59
60

Cold Month Mean (°C)

Page 45 of 47

Submitted to Phil. Trans. R. Soc. A - Issue

Terrestrial Surface Temperature (^{o}C)

a) PETM   Background Eocene Obs

Terrestrial Surface Temperature (^{o}C)

b) PRE-PETM   Background Eocene Obs

PETM Continental Clouds - PETM

Surface Temperature (°C)

PETM - PRE-PETM Precipitation Change (%)